ISSN 2395-6216 (PRINT VERSION)
ISSN 2395-6224 (ONLINE VERSION) Volume 13 Number 1 October 2022 - March 2023

Centurion Journal of Multidisciplinary Research

Centurion
UNIVERSITY

Shaping Lives...
Empowering Communities...

centurion university of technology and management

Centurion Journal of Multidisciplinary Research
ISSN 2395-6216 (PRINT VERSION) ISSN 2395-6224 (ONLINE VERSION)
https://cutm.ac.in/cjmr/centurion-journal-of-multidisciplinary-research/

Annual Subscription: Rs 300 (within India) excluding postage charges. Outside India USD 30, excluding postage charges. See website for details.

Published by:
Registrar, Centurion University of Technology and Management
R. Sitapur, Parlakhemundi, Gajapati, Odisha
Pin – 761211

Printer:
Srimandira Publication
EPF Colony, E-Block, Saheed Nagar, Bhubaneswar, Odisha 751007

Volume 13 Number 1
October 2022 to March 2023

Centurion Journal of Multidisciplinary Research

Centurion University
Shaping Lives...
Empowering Communities...

CENTURION UNIVERSITY PRESS, ODISHA, INDIA

About the Journal

Centurion Journal of Multi-disciplinary Research

Centurion Journal of Multi-disciplinary Research is a refereed journal, which serves as a platform for exploring the current issues, challenges and linkages in the broad areas of development, technology, engineering and management. There is a special focus on skill development and education, its recognition and promotion in the country, especially with the 'Make in India' initiative by the government of India. The objective of the journal is to facilitate bringing together research based contributions in science, technology, management and skills that has direct implication for the development of under-privileged communities and empowering them. The journal links theory and practice in the above areas so as to have policy and programme implications, particularly in under-developed contexts. In addition to articles from individuals or collectives, the journal publishes book reviews.

Aims and Scope of CJMR

CJMR is a multi-disciplinary, refereed journal serving as a forum for exploring theoretical and empirical understanding in the broad areas of development, management, science and technology. Perspective building in the area of skill development and education is another area which the journal would like to promote.

Centurion Journal of Multi-disciplinary Research aims at:

- Providing a platform for debate and dissemination of research findings, conceptual developments and new research areas and techniques that promise to change analyses and perspectives on science and technology, development, management, skill in developing societies;
- Disseminating and promoting research, good practice and innovation in all aspects of science, technology, management and skill development to its main audiences, including educators, researchers, graduate students, policy makers, and practitioners; and
- Encouraging multi-disciplinary cooperation and understanding, and enhancing quality research.

Volume 13 Number 1
October 2022 to March 2023

Centurion Journal of Multidisciplinary Research

Centurion Research Centers:
Shaping and Empowering through Knowledge...

In the journey of mankind from the caves to multitowered apartments, the search for knowledge has remained as the ultimate answer for humanity. May be in form of Gurukul or a university, academic institutions have always contributed to the pool of knowledge. They have answered to the queries of society through basic and applied research. Considering its responsibilities towards society, Centurion university of Technology and Management, has started 26 research centers to promote research to contribute to society in a better way. The youngest skill university of India has started its journey with the believe that these research centers will prove themselves useful for building a better tomorrow with the support and coordination from the academic community.

For more details on research centers:

Log on to : http://research.cutm.ac.in/

Name of the Research Centers

1. Center for 3DS Applications
2. Center for Agriculture Production
3. Center for AI & Robotics
4. Center for Aquaculture and Fish Processing Technology
5. Center for Chip Making
6. Center For Communication Technologies
7. Center for Computational Mathematics
8. Center for Data Sciences
9. Center for Digital Manufacturing
10. Center for Bioelectronics and Medical Systems
11. Center for Drug Design
12. Center for Edutech & Skilltech
13. Center for FinTech
14. Center for Governance and Sustainable Societies
15. Center for Genetics and Genomics
16. Center for Innovation and Entrepreneurship
17. Center For LASER
18. Center for Medical Diagnostics
19. Center For Manufacturing
20. Center for New Material Applications
21. Center for Phytopharma
22. Center for Smart Mobility and Machines
23. Center for Waste to Wealth Management
24. Center for Smart Infrastructure
25. Centre for Space and Earth Sciences
26. Center for Smart Agriculture

Volume 13 Number 1
October 2022 to March 2023

Centurion Journal of Multidisciplinary Research

Editorial

kkkkkkkkkkkkkkkkkkkkkkkkkkkkkkkkkkkk
kkkkkkkkkkkkkkkkkkkkkkk

kkkkkkkkkkkkkkkkk

Volume 13 Number 1
October 2022 to March 2023

Centurion Journal of Multidisciplinary Research

Chief Editor

Contents

Articles

Temperature dependent dielectric and electrical characteristics of rare earth substituted SBT ceramic

G. K. Sahu, S. Parthasarathy and S. Behera 1

Theoretical study on the Lead-Free Perovskite Materials for the Application in Photovoltaic Cells

Priyambada Mallick, Santosh Ku. Satpathy and Susanta Ku. Biswal 24

Chitosan nanocomposites in dental application

Himanshu B Samal, Nigam S Tripathy, Liza Sahoo and Fahima Dilnawaz 31

Investigation of Antipshycotic Activity of Ethano Medicinal Plants of Cucurbitaceae Family

Trayambica Acharya, Ashirbad Nanda and Rupali Rupasmita Rout 45

Thermodynamic properties of ternary liquid mixtures containing N-N dimethylformamide (DMF), Cyclohexane and Chloro-benzene at different frequencies

Manoj Kumar Praharaj and Subhraraj Panda 59

Smart Ways of Biomaterial Designing: A Comprehensive Review

Ashirbad Nanda, Rudra Narayan Sahoo, Bikash Ranjan Jena and Smruti Smaranika Sahoo 69

Thermodynamic Parameters and Their Excess Values for Binary Mixtures of Cyclohexane and Substituted Benzenes at different frequencies

Manoj Kumar Praharaj and Subhraraj Panda 87

Temperature dependent dielectric and electrical characteristics of rare earth substituted SBT ceramic

Centurion Journal of
Multidisciplinary Research
ISSN: 2395 6216 (PRINT VERSION)
ISSN: 2395 6224 (ONLINE VERSION)
Centurion University of Technology
and Management
At - Ramchandrapur
P.O. - Jatni, Bhubaneswar
Dist: Khurda – 752050
Odisha, India

G. K. Sahu[1], S. Parthasarathy[1] and S. Behera[1*]

Abstract

The $Sr(Bi_{0.9}Y_{0.1})_2Ta_2O_9$ ceramic was prepared by standard SSR method at an optimized calcination temperature (1000^0C). Formation of single-phase compound with orthorhombic crystal structure is confirmed from XRD pattern. The temperature variation of dielectric constant exhibits improved thermal stability (TCC) behaviors useful for MLCC applications. The room temperature hysteresis loop confirms the ferroelectric property of the material with good remnant polarization applicable for memory device. Complex impedance spectroscopy is

[1] Department of Physics, Centurion University of Technology and Management, Odisha, India.

* Corresponding Author, Email: saubhagyalaxmi.behera@cutm.ac.in, mamisana1410@gmail.com, Ph-9438108634

used to determine the distinct components in the corresponding electrical circuit. The fact that ac conductivity changes with temperature indicates that the conduction mechanism is a thermally triggered process. Conduction occurs in the ceramics due to the long-range mobility of single -ionized oxygen vacancies. The thermistor parameters are calculated at higher temperature for NTC thermistor applications.

Keywords: Dielectric; X-ray diffraction; TCC, Complex Impedance; Ferroelectricity; Thermistor.

1. Introduction

Ferroelectrics with Bismuth layered structure like $SrBi_2Ta_2O_9$ (SBT), $SrBi_2Nb_2O_9$ (SBN) are important materials for temperature stable memory devices (FRAMs) [1-6]. In particular, SBT is widely explored due to its excellent properties like extended cycling with polarization fatigue reduced or alleviated polarization fatigue up to 10^{12} cycles, low switching voltage, good ferroelectric properties (large P_r values) and low leakage current [2]. It is known that by suitable stoichiometric change in both bulk and thin film of SBT ceramics, the dielectric and ferroelectric properties can be modified [7,8]. Some groups have attempted to improve the remnant polarization of SBT ceramic by modifying the composition[9,10]. Senthil *et al.* reported the effect of rare earth Y^{3+} substitutions in Sr^{2+} site on the ferroelectric, electrical and photocatalytic behavior of SBT ceramics[11]. The improvement of ferroelectric behavior of SBT ceramics by rare-earth doping in and is also reported by others [12,13]. In literature it is known that the ferroelectric and electrical behaviors of BLSF structures are strongly determined by layers. The modifications in dielectric and ferroelectric properties of SBT ceramic by appropriate replacement of ions by lanthanide cations are explored earlier [14]. Some efforts are also reported on the rare earth doping on Bi sites for LED applications [15,16]. So, it is concluded that rare-earth doping in the Bi sites is

effective for improvement of useful properties. This paper discusses the characteristics behaviour of Yttrium () substituted SBT ceramic. We have adopted a trial method by slowly increasing the calcination temperature followed by phase conformation after each interval to optimize the minimum formation temperature.

2. Experimental methods

The high purity oxides (>99.9%): $SrCO_3$, Bi_2O_3, Y_2O_3 and Ta_2O_5 are used as starting raw materials which are weighed according to the stoichiometric ratio with the $Sr(Bi_{0.9}Y_{0.1})_2Ta_2O_9$ abbreviated as SBYT and ground in an agate mortar for 2 h. The mixed powder is ball milled in a laboratory ball milling machine using Zr ball in acetone medium. 3 wt% of excess Bi_2O_3 is added with calculated precursors to compensate the loss during sintering. The mixed precursors are calcined at 1273K for 4 h after drying acetone. Then the calcined powder is ground in agate mortar and mixed with polyvinyl alcohol (PVA) (Merck KGaA, 64271 Darmstadt.) which act as a binder for preparation of the disk. The powder is uniaxially pressed into circular disks of 10-12 mm in diameter and 1-1.5 mm in thickness and sintered at 1473K for 1 h with a heating rate of 5K/min. The end faces of the sintered pellets are made parallel and flat using fine emery paper. The phase formation of the sintered pellets is structurally characterized using X-ray diffraction (XRD) (PANalytical, Japan) and surface morphology of the sintered pellet is studied using Scanning electron microscope, (JEOL, USA). In order to measure the electrical properties, disk surfaces are polished uniformly and coated with silver paste (Coatex Industries) for electroding purpose. After electroding the pellet was dried for 1 h at 473K to remove the moisture if present and was cooled to room temperature before taking any electrical measurement. Temperature dependence dielectric data are measured from 300K to 673K with the rising temperature of 1K/min using Salatron 1260 gain/phase analyzer, Germany. The hysteresis is studied using P–E loop tracer (Radient Technology, USA).

3. Result and Discussion

3.1. Structural and morphological analysis

The XRD pattern of the sintered pellet of SBYT ceramic is presented in Figure 1. The observed peaks and lattice parameter were redefined using X'Pert high score computer Software program. The XRD analysis reveal the grown materials have single-phase Bi-layered () Aurivillius compounds with orthorhombic symmetry, which is consistent with standard XRD database (JCPDS: 49-0609). The sharp and distinguished peaks confirm the formation of new single-phase material. The derived lattice parameters are and . In the XRD patterns, a strong (115) diffraction line at about 28.39° is detected, which indicates polarization along the a-axis direction [11].

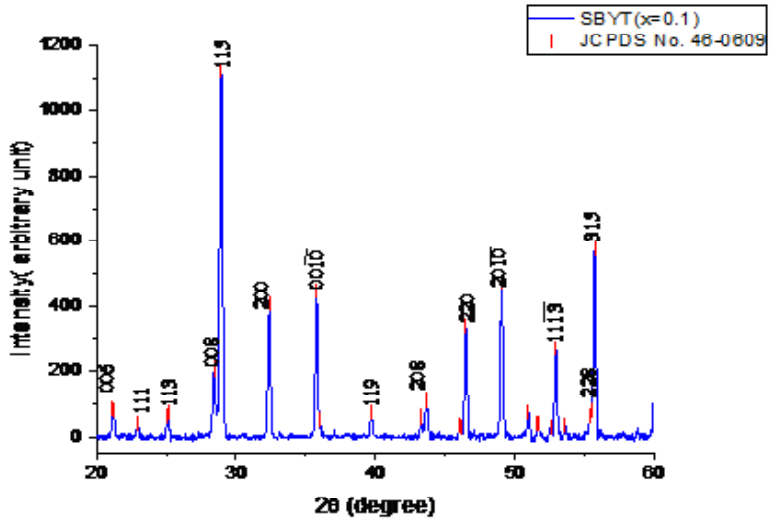

Figure 4.1: XRD patterns of the SBYT ceramic (x=0.1)

3.2 Microstructural Analysis

Figure 2 gives the surface morphology of the sintered pellet of Y substituted SBT ceramic. The distinctive features of bismuth layer compounds are clearly observed from the grain morphologies of the ceramic. The sample exhibits anisotropy, and the grains have a rod-like shape with minimal porosity. The bulk density of sintered pellets is found to be 95-97% of the theoretical density. The SEM micrographs manifest the polycrystalline nature of the SBYT ceramics.

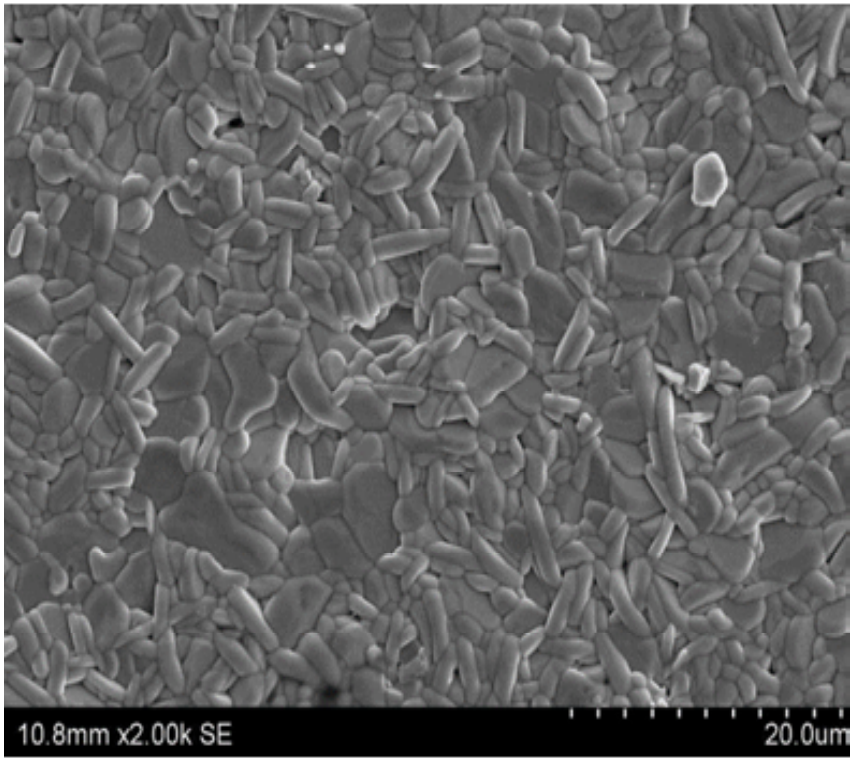

Figure 2: Surface morphology of the SBYT ceramic

3.3. Dielectric properties

The dielectric permittivity (ε_r) of SBYT ceramic varies with temperature (Figure 3) at selected frequencies in a similar behaviour of other Bismuth layered structure ferroelectrics [17-20].The reduction in both dielectric constant and ferroelectric phase transition with the substitution excess amount of Yttrium is an indication of the development of ionic bond (Y–O) from covalent bond (Bi–O) in the Bi_2O_2 layer [21]. Additionally, the lowering of both the dielectric parameters (and) is explained in terms of reduction of octahedron distortion of SBT ceramics.The unit cell dimension and lattice deviation of the parent SBT ceramic increases because of incorporation of the cation having a larger covalent radius as compared to .The lone pair of $6s^2$ electrons present in ion actively participate in induction of dipole moment (polarization) in the perovskite layers of SBT structure as compared to bonded electron pairs. Consequently, the absenteeism of lone pair of electrons in the lanthanide cation () reduces the net induced polarization and B site octahedral distortion. Again, according to Shannon (1993) the room temperature polarizability for is more than . From Clausius- Mossotti relation the lower polarizability will shift the and lower temperature site.Again, it is also stated that doping with small cationic radius in A site of SBT ceramics creates more rattling space resulting more dielectric constant with high transition temperature although amalgamation of large ionic radius fallouts a converse effect [22,23]. So, both the maximum dielectric constant () and transition temperatures () fall down with substitution of Y. Lowering of maximum dielectric constant values with doping has a noteworthy effect on improvement of remnant polarization in SBT based ceramics useful for memory applications. The frequency dependent or strict relaxor behaviour is not observed in the composition because of absence of nano sized polar regions (PNR) in them resulting from their large grain size. As it is known that this PNR are responsible for relaxor behavior in Bi based perovskites [24]

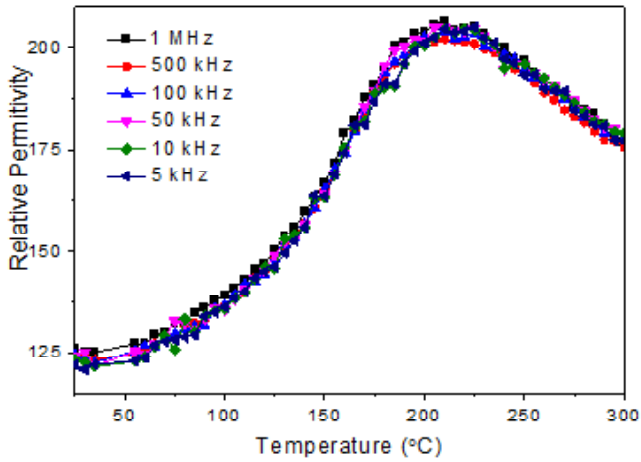

Figure 3: Temperature variation of dielectric constant at various frequency

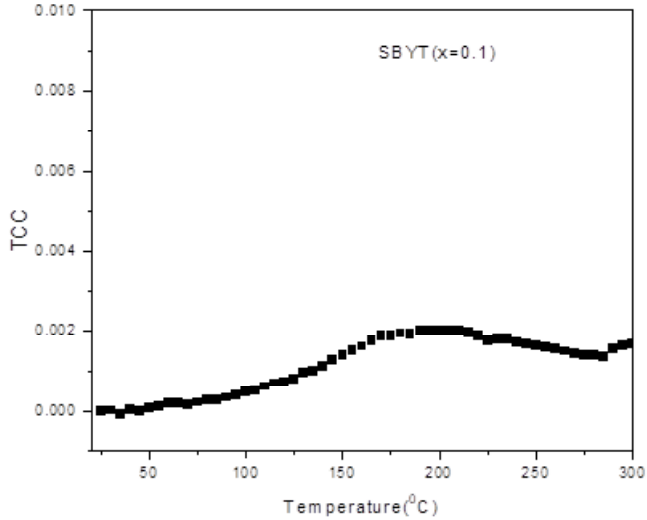

Figure 4: Variation of TCC of SBYT ceramic with temperature at 50 KHz

The dielectric constant of the Y modified ceramic shows negligible variation with temperature up to 300^{0}C indicating excellent thermal stability. The thermal stability of the materials is related to the capacitance (C) and is expressed by the temperature coefficient of capacitance (TCC). The temperature coefficient of dielectric constant TCC ($\hat{o}_{\mathring{a}}$) is calculated using the formula

$$\tau_{\varepsilon} = (\varepsilon_T - \varepsilon_{RT})/\varepsilon_{RT}\Delta T$$

where ÄT =measuring temperature (T)-room temperature (RT) and $\mathring{a}_{RT}$ is the room temperature dielectric constant. The units of TCC is parts per million (ppm)°C^{-1} and TCC H" 0 indicates high thermal stability of the materials as capacitors. The TCC was calculated for the sample within temperature range (25-300)^{0}C and presented in Fig. 4. In the above temperature range the values of $\hat{o}_{\mathring{a}}$ are close to zero which reflects the suitability of the materials for microwave resonators and MLCC application.

The broad dielectric peaks specify the presence of second order phase transitions in these materials with broadening confirmed by conniving the degree of diffuseness ($\tilde{a}$) from the temperature variation of dielectric constant using the modified Curie–Weiss law [25]:

$$\frac{1}{\varepsilon} - \frac{1}{\varepsilon_{\mathrm{m}}} = \frac{(T - T_{\mathrm{m}})^{\gamma}}{C'} \qquad (\text{at } T > T_m) \qquad (4.1)$$

where C' is a constant, γ has values between 1 and 2. The values of indicate classical Curie Weiss law and an ample diffuse phase transition respectively. The corresponding $\tilde{a}$ values are calculated from the slopes of the plot between logarithm of () and logarithm of () at 50 kHz (Figure 5).

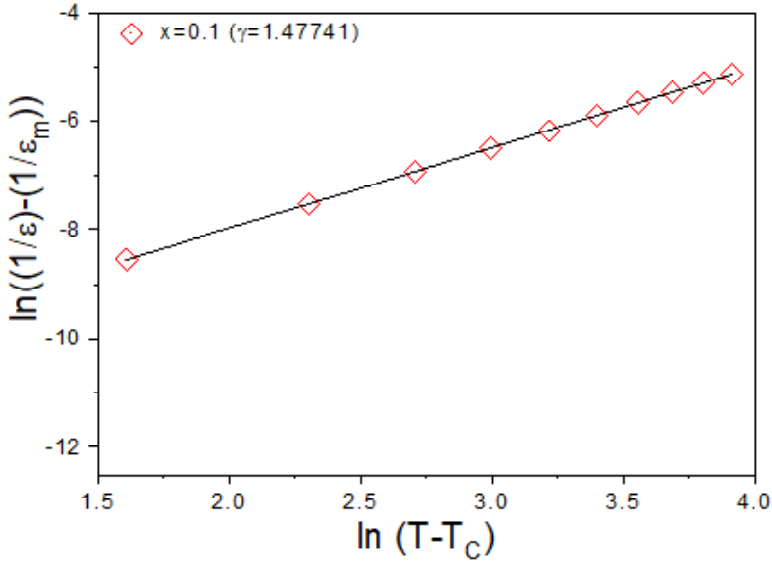

Figure 5: Relationship between logarithm of $(1/\varepsilon - 1/\varepsilon_m)$ and logarithm of $(T - T_C)$ at 50 kHz for SBYT ceramic.

The presence of more than two no of cations in the A site of the perovskite layers is responsible for such type of phase transition in it. It is also reported earlier that doping of rare earths in Bi-site of BLSF structure predisposed the dielectric constant with wide peak because of the nonuniform dispersal of rare earths in layered structure [26,27]. The presence of diffuse phase transition in the material is confirmed from the values of ã (degree of diffusivity) as 1.47 (between 1 to 2).

3.4 Ferroelectric properties

The assumed ferroelectric behaviour of the Yttrium modified SBT ceramic is confirmed from the polarization reversal curves (hysteresis loop) shown in Figure 6.The closed hysteresis loop in this figure confirms the assumed ferroelectric nature in the dielectric plot. The observed

good remnant polarization (P_r) in the material aligns it for memory applications. In the process of high temperature sintering stoichiometric loss occurs in the pure SBT material due to volatilization of Bi_2O_3 leaving some oxygen vacancies in terms of inherent defects [28]. Substituting an isovalent lanthanoid cation for Bi^{3+} at the A-site reduces bismuth vacancies and stabilises oxygen ions in the perovskite layers [29]. These oxygen vacancies (V_o) work as space charge resulting strong pinning of the domains causing less values [30,31]. With the addition of the trivalent ion (), to maintain the structure's overall charge neutrality, cation vacancies are produced in the A-site. Hence the dopant ion behaves as a donor reducing the oxygen vacancies and the pinning effect on the domain walls with a larger contribution of to the parent materials [32]. It is also anticipated that the polarization increases due to doping as a result of increase of no of switchable domain in the presence of electric field [6].

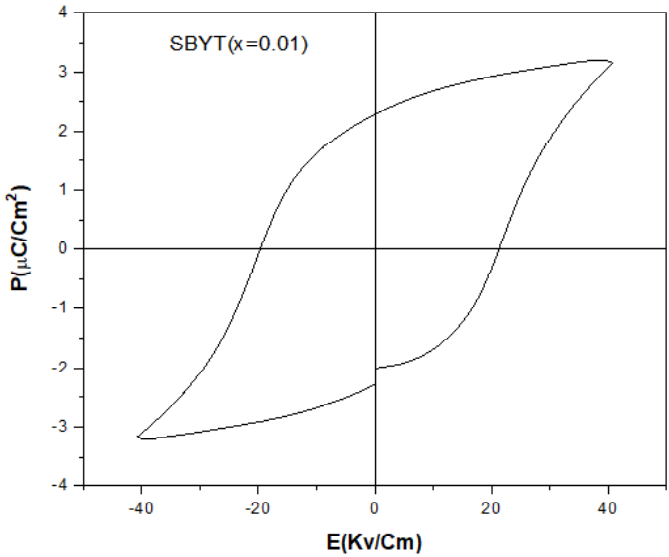

Figure 6: The P–E hysteresis loops of SBYT ceramic.

3.5 AC conductivity

The AC conductivity of SBYT ceramic as function of frequency (5kHz-1MHz) at different temperatures is shown in Figure 7. The graph is divided into three sections with varying slopes: (i) low frequency dispersion, (ii) intermediate frequency (plateau) dispersion, and (iii) high frequency conductivity dispersion. In the low frequency (space-charge) region, the polarisation effect causes variations in conductivity. The long-range translational motion of ions contributing to dc conductivity (σ_{dc}) is ascribed to the frequency independent plateau at moderate frequency [33]. The charts show that the material's conductivity increases as the temperature rises. Also, the dispersion is readily evident at lower frequencies, while the curves blend at higher frequencies. In the high frequency range, however, conductivity rises at all temperatures when the slope changes. The hopping frequency is the rate at which the slope varies. With rising temperature, the hopping frequency changes to the upper side, as seen in the graph [34]. As the temperature rises, a frequency independent zone (plateau region) stretches to the higher frequency and relaxes into a strong dispersive region. The plateau zone results from long-range charge carrier movement, while the dispersive region results from localised or short-range charge carrier movement, resulting in ac conduction. As a result, the relaxation frequency is determined by the point at which dc to ac conduction occurs [35]. Jonscher's power law [36] governs this kind of frequency dependent conductivity s(u) spectrum:

$$\sigma_{ac} = \sigma_{dc} + A\omega^n \qquad (4.2)$$

where is the DC conductivity (corresponding to the frequency-independent plateau in the low-frequency region), is a frequency pre-exponential factor which depends on temperature, and is the power-law exponent (). The preexponential factor (A) controls the intensity

of the polarizability, whereas the power n denotes the degree of interaction between mobile ions and the lattice surrounding them. It is clear that rises with frequency, although it is practically independent in the low-frequency area. is obtained by extrapolating this component towards the lower frequency side. The rising tendency of with increasing frequency (in the low frequency area) might be explained by cation disorder between surrounding sites or the existence of space charge [37]. The curves approach each other in the high-frequency area. A low-frequency dispersion phenomenon following Jonscher's power law is shown by the conductivity charts. The origin of the frequency dependence of conductivity, according to Jonscher, is related to relaxation events caused by mobile charge carriers. A mobile charge carrier stays in a condition of displacement between two potential energy minima as it hops to a new site from its initial location.

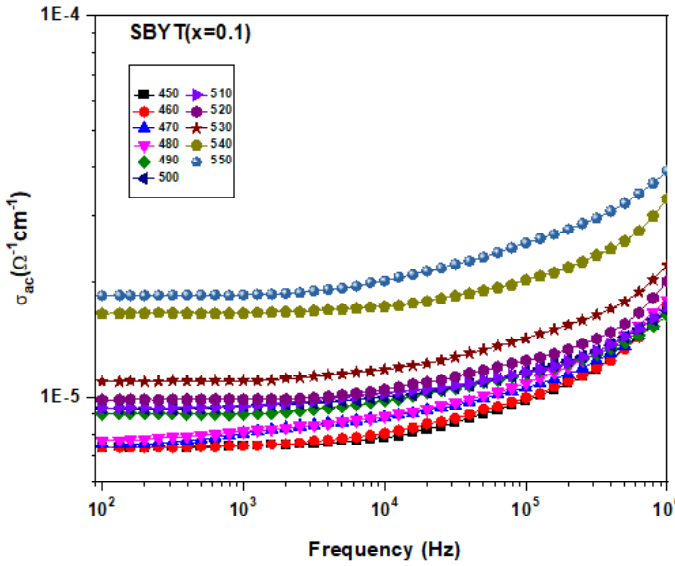

Figure 7: Frequency dependence AC conductivity at different temperature for SBYT ceramic.

3.6 Complex impedance analysis

Impedance spectroscopy is a good way to link the electrical properties of heterogeneous polycrystalline materials to their microstructure. The complex impedance (Z) is generally expressed as:

$$Z = Z' + jZ'' \qquad (1)$$

where Z' and Z'' are the resistive and the reactive part of the impedance. This section describes the frequency and temperature dependent components of impedance for the material. The numerous contributions made in the system can be quantified by fitting the impedance data with an analogous electrical circuit. Figures 8(a &b) demonstrate the frequency dependent real impedance () and imaginary impedance () for SBYT ceramic at the temperature range of 450-550°C. Because of the release of space charge induced by a decrease in barrier characteristics as temperature rises, the Z' values for all temperatures blend at a high frequency. It could also explain why ac conductivity rises with temperature at high frequencies. When the frequency (log f) is increased, the Z' falls, suggesting an increase in AC conductivity. Furthermore, the nonlinear behaviour of Z' values as a function of temperature is evident. The asymmetric fluctuation in the broadness of the Z'' peaks pointed to an electrical process with a relaxation time spread [38]. The presence of temperature dependent relaxation phenomenon is explained by the shifting of Z'' max towards the high frequency side. The reduction in Z'' with temperature shows increased conductivity due to the material's space charge. Because it takes less time for space charges to relax and recombine at high frequencies, space charge polarization decreases as frequency rises and seems to merge at high frequencies for all temperatures.

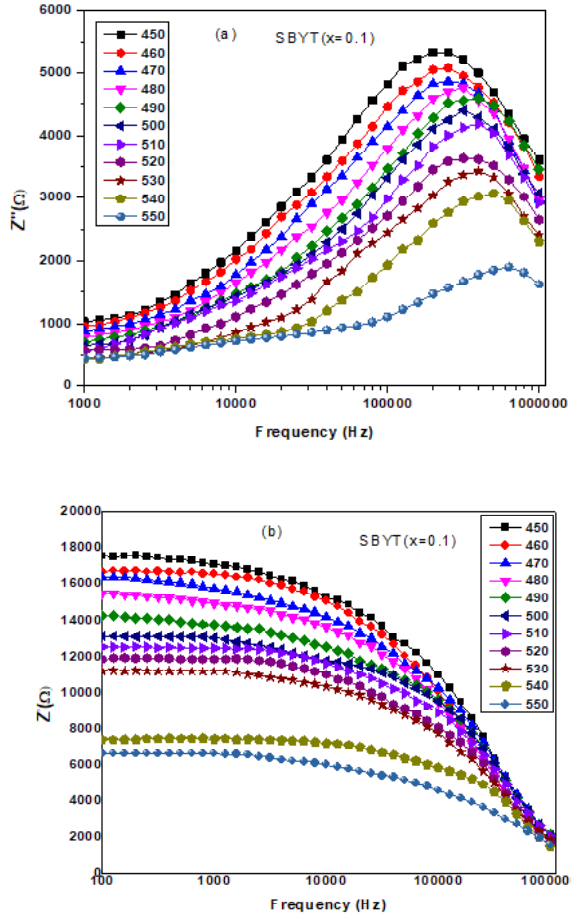

Figure 8: Variation of impedance with frequency at different temperatures for SBYT **(a)** imaginary value of impedance (Z3) **(b)** real value of impedance (Z').

For polycrystalline materials, complex impedance spectroscopy is utilized to investigate frequency domain features (such as grain, grain boundary, and interface effects). The qualitative information regarding the contribution of grain, grain boundary, and interface effects is provided

over a wide range of frequencies and temperatures. Utilizing applicable equations, one can anticipate the theoretical values of a material by using a parallel combination of resistance (R) and capacitance (C) in an equivalent electrical circuit. The fitting of impedance spectroscopy data to an equivalent electrical circuit can reveal how the system's various contributions evolved. In an analogous circuit, each parallel combination of $R - C$ must be considered for its own relaxation process.

The complex impedance spectrum (Z' vs Z") of SBYT ceramic is shown in Figure 9. The sample fits best with a series of two parallel components $RC - RQ$ or $RQ - RC$, where " is resistance," is capacitance, and " is the constant phase element (CPE) indicating the electrical contributions from both grain and grain boundary[39-40] (equivalent circuit is drawn on the graph). The term CPE refers to a relaxation mechanism that is not Debye, in which the centre of a semicircle is dislocated below the axis. With increasing temperature, the radius of the semicircle shrinks, confirming the negative temperature coefficient of resistance of the material. Fig 10 shows the fitting parameters (bulk resistance) as a function of temperature for the complex impedance spectrum using SBYT ceramics equivalent circuits.

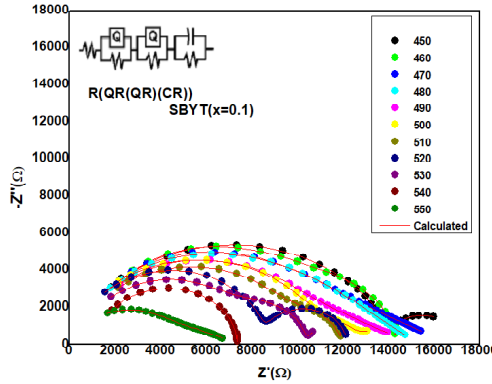

Figure 9: Complex impedance spectrum (Z2 vs Z3) of SBYT ceramic (Solid line represents respective circuit fitting).

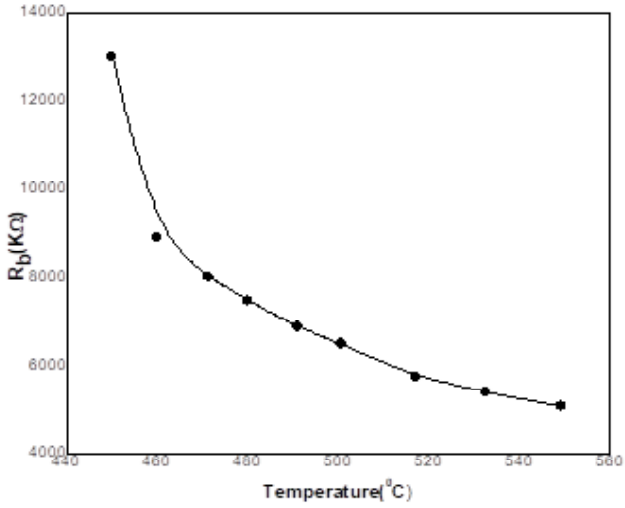

Figure 10:Variation of bulk resistance with temperature of the ceramic.

3.7 Thermistor Constant beta (β) or Sensitivity

It is noticed from the temperature variation of bulk resistance (Fig.10) graph that resistance follows semiconductor behavior with increasing temperature by the following exponential equation.

$$R = R_0 \exp\left(\frac{-E_a}{K_B T}\right) \quad \text{or} \quad R = R_0 \exp\beta\left(\frac{1}{T} - \frac{1}{T_0}\right) \qquad (1)$$

Where R and R_0 are the resistance of the compound at the temperature T (K) and fixed temperature T_0(K) respectively and β is material characteristic properties known as the NTC thermistor parameter.

The following equation is used to get the value

$$\beta = \frac{ln\left(\frac{R_{T1}}{R_{T2}}\right)}{\left(\frac{1}{T_1} - \frac{1}{T_2}\right)} \qquad (2)$$

Where and are the resistances at two different temperature T_1 and T_2 respectively. The thermistor specification and components are decided from the values of [41]. The variation of with temperature is shown in fig.11 and it directly varies with the temperature. In literature it is open that should ranges between 4000K-15000K for use as good thermal sensor [42]. The values of calculated for the material remain between 6000K-116000K and concludes the use of the material as high temperature NTC thermistor.

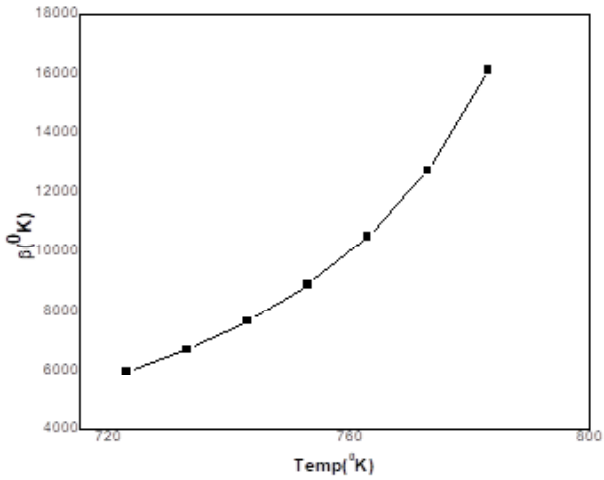

Fig.11: Variation of β with temperature.

4. Conclusion

The $Sr(Bi_{0.9}Y_{0.1})_2Ta_2O_9$ ceramic was prepared by standard SSR method. Formation of single-phase compound with orthorhombic structure is confirmed from XRD pattern. The temperature variation of dielectric constant exhibits improved dielectric behaviours with lower transition temperature values near room temperature device applications. The room temperature hysteresis loop confirms the ferroelectric property of the material with good remnant polarization applicable for memory

device. Complex impedance spectroscopy is used to determine the distinct components in the corresponding electrical circuit. Conduction occurs in doped ceramics due to the long-range mobility of single - ionized oxygen vacancies. The study of temperature-dependent resistance supports SBYT as a good candidate for NTC thermistor-related device applications. The frequency variation of ac conductivity follows Josher's power law. The negligible TCC value of the material is promising for a tunable microwave device.

REFERENCES

[1] Kajewski, D. and Ujma, Z. (2013) .Electrical conductivity of $SrBi_2Ta_2O_9$ ceramics. Ceramics International, 39 (7), 8213-8218.

[2] Coondoo, I. and Jha, A. K., (2009). Enhancement of ferroelectric and piezoelectric characteristics in europium substituted $SrBi_2Ta_2O_9$ ferroelectric ceramics. Materials Letters ,63 (1), 48-50.

[3] Kajewski, D. and Ujma, Z. (2010). Electrical properties of $SrBi_2(Nb_{0.5}Ta_{0.5})_2O_9$ ceramics. Journal of Physics and Chemistry of Solids ,71 (1), 24-29.

[4] Senthil, V., Badapanda, T., Chithambararaj, A., Chandra Bose, A., and Panigrahi S. (2016). Impedance spectroscopy and photocatalysis water splitting for hydrogen production with cerium modified $SrBi_2Ta_2O_9$ ferroelectrics. International Journal of Hydrogen Energy, 41 (48), 22856-22865.

[5] Chen, Y., Du, Y., Fan, D., Niu, H., Zuo, Y., Hu, L., Liu, K., Shen, M., Shang, X., and Chen, Y. (2021) Study on the polarization enhancement mechanism and electrical properties of high temperature bismuth layered $K_xNa_{0.5-x}Bi_{4.46}Ce_{0.04}Ti_4O_{15+y}$ ceramics. Ceramics International, 47 (20), 29023-29029.

[6] Chen, Y., Zhang, C.-C., Qin, L., Jiang, C.-B., Liu, K.-H., Ma, C., Wu, Z.-T., Pan, R.-K., Cao, W.-Q., Ye, C., and Li, Z.(2018). Enhanced

dielectric and piezoelectric properties in $Na_{0.5}Bi_{4.5}Ti_4O_{15}$ ceramics with Pr-doping. Ceramics International, 44 (15), 18264-18270.

[7] Coondoo, I., Jha, A. K. and Agarwal, S. K. (2007). Structural, dielectric and electrical studies in tungsten doped $SrBi_2Ta_2O_9$ ferroelectric ceramics. Ceramics International ,33 (1), 41-47.

[8] Wang, D.-S. (2014). Effect of annealing atmosphere on volatility of Bi in $SrBi_2Ta_2O_9$ thin films," J Ceram Process Res, 15 (2), 116-119.

[9] Kitamura, A., Noguchi, Y., and Miyayama, M. (2004). Polarization properties of praseodymium-modified $SrBi_2Ta_2O_9$ ceramics and thin films prepared by sol–gel method. Materials Letters, 58 (11), pp. 1815-1818.

[10] Sridarane, R., Subramanian, S., Janani, N., and Murugan, R. (2010). Investigation on microstructure, dielectric and impedance properties of $Sr_{1-x}Bi_{2+(2/3)x}(V_xTa_{1-x})_2O_9$ [x=0, 0.1 and 0.2] ceramics. Journal of Alloys and Compounds, 492 (1), 642-648.

[11] Senthil, V. and Panigrahi, S. (2019). Dielectric, ferroelectric, impedance and photocatalytic water splitting study of Y^{3+} modified $SrBi_2Ta_2O_9$ ferroelectrics. International Journal of Hydrogen Energy, 44 (33), 18058-18071.

[12] Wei, T., Zhao, C. Z., Zhou, Q. J., Li, Z. P., Wang, Y. Q., and Zhang, L. S. (2014). Bright green upconversion emission and enhanced ferroelectric polarization in $Sr_{1-1.5x}Er_xBi_2Nb_2O_9$. Optical Materials, 36 (7), 1209-1212.

[13] Sugandha and Jha, A. K. (2013). Effect of holmium substitution on electrical properties of strontium bismuth tantalate ferroelectric ceramics. Ceramics International, 39 (8), 9397-9403.

[14] Senthil,V., Badapanda,T., Chandrabose,A., and Panigrahi, S. (2015). Dielectric and ferroelectric behavior of cerium modified $SrBi_2Ta_2O_9$ ceramic. Materials Letters, 159, 138-141.

[15] Zhong,Y., Sun, P., Gao, X., Liu, Q., Huang, S., Liu, B., Deng, B., and Yu, R.(2019). Synthesis and optical properties of new red-emitting $SrBi_2Ta_2O_9:Eu^{3+}$ phosphor application for w-LEDs commercially based on InGaN. Journal of Luminescence , 212, 45-51.

[16] Zhong, Y., Deng, B., Gao, X., Sun, P., Ren, Y., Liang, T., and Yu, R. (2019). High thermally Sm^{3+}-activated $SrBi_2Ta_2O_9$ orange-red phosphor: Preparation, characterization, and optical properties. Journal of Luminescence , 215, 116648 .

[17] Nayak, P., Badapanda, T., and Panigrahi, S. (2016). Dielectric and ferroelectric properties of Lanthanum modified $SrBi_4Ti_4O_{15}$ ceramics. Materials Letters, 172, 32-35.

[18] Sahu, R. and Kumar, P. (2020). Microstructural, dielectric and ferroelectric properties of $Sr_{0.8}Bi_{2.15}Ta_2O_9$ ceramics synthesized by microwave processing technique. Phase Transitions 93 (1), 91-99.

[19] Nayak, P., Badapanda, T., and Panigrahi, S. (2017). Effect of lanthanum modification on dielectric and conduction behaviour of $SrBi_4Ti_4O_{15}$ ceramic. AIP Conference Proceedings, 1832 (1), 030017.

[20] Miyayama, M. and Noguchi, Y. (2005). Polarization properties and oxygen-vacancy distribution of $SrBi_2Ta_2O_9$ ceramics modified by Ce and Pr. Journal of the European Ceramic Society, 25 (12), 2477-2482.

[21] Zhu, J. S., Qin, H. X., Bao, Z. H., Wang, Y. N., Cai, W.Y., Chen, P. P., Lu, W., Chan, H. L. W., and Choy, C. L. (2001). X-ray diffraction and Raman scattering study of $SrBi_2Ta_2O_9$ ceramics and thin

films with Bi_3TiNbO_9 addition.Applied Physics Letters ,79 (23), 3827-3829.

[22] Verma, M., Sreenivas, K., and Gupta, V. (2009). Influence of La doping on structural and dielectric properties of $SrBi_2Nb_2O_9$ ceramics. Journal of Applied Physics, 105 (2), 024511 .

[23] Sun, L., Feng, C., Chen, L., and Huang, S. (2007). Dielectric and Piezoelectric Properties of $SrBi_{2-x}Sm_xNb_2O_9$ (x=0, 0.05, 0.1, 0.2, 0.3, and 0.4) Ceramics. Journal of the American Ceramic Society, 90 (12), 3875-3881 .

[24] Praharaj, S., Rout, D., Anwar, S., and Subramanian, V. (2017). Polar nano regions in lead free $(Na_{0.5}Bi_{0.5})TiO_3$-$SrTiO_3$-$BaTiO_3$ relaxors: An impedance spectroscopic study. Journal of Alloys and Compounds ,706, 502-510 .

[25] Park, B. H., Hyun, S. J., Bu, S. D., Noh, T.W., Lee, J., Kim, H.-D., Kim, T. H., and Jo, W. (1999) Differences in nature of defects between $SrBi_2Ta_2O_9$ and $Bi_4Ti_3O_{12}$. Applied Physics Letters, 74 (13), 1907-1909 .

[26] Afqir, M., Tachafine, A., Fasquelle, D., Elaatmani, M., Carru, J.-C., Zegzouti, A., Daoud, M., Sayouri, S., Lamcharfi, T.-D., and Zouhairi, M. (2018). Structural, electric and dielectric properties of Eu-doped $SrBi_2Nb_2O_9$ ceramics obtained by co-precipitation route. Processing and Application of Ceramics , 12 (1), 72- 77.

[27] Adak, M. K., Mukherjee, A., Chowdhury, A., Khatun, J., Dhak, P., and Dhak, D. (2019). Dielectric anomaly, diffusivity and impedance behavior of transition metal substituted $SrBi_2NbTaO_9$ ferroelectric nano-ceramics prepared by chemical route. Physica B: Condensed Matter, 553, 26-35.

[28] Kannan, B. R. and Venkataraman, B. H. (2014). Effect of rare earth ion doping on the structural, microstructural and diffused phase transition characteristics of $BaBi_2Nb_2O_9$ relaxor

ferroelectrics. Ceramics International, 40 (10, Part B), 16365-16369.

[29] Gupta, P., Mahapatra, P. K., and Choudhary, R. N. P. (2018). Structural and Electrical Characteristics of an Aurivillius Family Compound $Bi_2LaTiVO_9$. Crystal Research and Technology, 53 (12), 1800045.

[30] Noguchi, Y., Miwa, I., Goshima, Y., and Miyayama, M. (2000). Defect Control for Large Remanent Polarization in Bismuth Titanate Ferroelectrics — Doping Effect of Higher-Valent Cations. Japanese Journal of Applied Physics, 39 (Part 2, No. 12B), L1259-L1262.

[31] Friessnegg, T., Aggarwal, S., Ramesh, R., Nielsen, B., Poindexter, E. H., and Keeble, D. J. (2000). Vacancy formation in $(Pb,La)(Zr,Ti)O_3$ capacitors with oxygen deficiency and the effect on voltage offset. Applied Physics Letters, 77 (1), 127-129 .

[32] Coondoo, I. and Jha, A. K. (2007). Investigations of structural, dielectric and ferroelectric behavior of europium substituted $SrBi_2Ta_2O_9$ ferroelectric ceramics. Solid State Communications, 142 (10), 561-565 .

[33] Li, W. and Schwartz, R. W. (2006). ac conductivity relaxation processes in $CaCu_3Ti_4O_{12}$ ceramics: Grain boundary and domain boundary effects. Applied Physics Letters, 89 (24), 242906 .

[34] Srinivas, K., Sarah, P., and Suryanarayana, S.V. (2003). Impedance spectroscopy study of polycrystalline $Bi_6Fe_2Ti_3O_{18}$. Bulletin of Materials Science, 26 (2), 247-253 .

[35] Pattanayak, R., Panigrahi, S., Dash, T., Muduli, R., and Behera, D. (2015). Electric transport properties study of bulk $BaFe_{12}O_{19}$ by complex impedance spectroscopy. Physica B: Condensed Matter, 474, 57-63 .

[36] Jonscher, A. K. (1977). The 'universal' dielectric response. Nature, 267 (5613), 673-679 .

[37] Karan, N. K., Pradhan, D. K., Thomas, R., Natesan, B., and Katiyar, R. S. (2008). Solid polymer electrolytes based on polyethylene oxide and lithium trifluoro- methane sulfonate (PEO–$LiCF_3SO_3$): Ionic conductivity and dielectric relaxation. Solid State Ionics, 179 (19), 689-696 .

[38] Khokhar, A., Mahesh, M. L. V., James, A. R., Goyal, P. K., and Sreenivas, K. (2013). Sintering characteristics and electrical properties of $BaBi_4Ti_4O_{15}$ ferroelectric ceramics. Journal of Alloys and Compounds, 581, 150-159 .

[39] Gupta, P., Mahapatra, P. K., and Choudhary, R. N. P. (2021). Structural and electrical characteristics of rare-earth modified bismuth layer structured compounds. Journal of Alloys and Compounds, 863, 158457 .

[40] Badapanda, T., Nayak, P., Mishra, S. R., Harichandan, R., and Ray, P. K. (2019). Investigation of temperature variant dielectric and conduction behaviour of strontium modified $BaBi_4Ti_4O_{15}$ ceramic. Journal of Materials Science: Materials in Electronics, 30 (4), 3933-3941 .

[41] Luo, W., Yao, H. M., Yang, P.H. (2009). Negative temperature coefficient material with low thermal constant and high resistivity for low temperature thermistor applications. J Am Ceram Soc, 92, 2682–2686.

[42]. Mott, N.F. (1990). Metal insulator transitions. London: Taylor and Francis.

Theoretical study on the Lead-Free Perovskite Materials for the Application in Photovoltaic Cells

Centurion Journal of
Multidisciplinary Research
ISSN: 2395 6216 (PRINT VERSION)
ISSN: 2395 6224 (ONLINE VERSION)
Centurion University of Technology
and Management
At - Ramchandrapur
P.O. - Jatni, Bhubaneswar
Dist: Khurda – 752050
Odisha, India

Priyambada Mallick[1], Santosh Ku. Satpathy[1] * and Susanta Ku. Biswal[1]

Abstract

Perovskite PV cells with better open-circuit voltage and high efficiency of power conversion attracted much more attention from scientists and researchers due to the rapid improvement in the performance and efficiency of PV cells. Some appropriate halide perovskites such as Ge- based halide, Bi-based halide, Sb-based halide and Sn-based halide can be used in the place of Lead due to the low cost, less/non-toxicity, high stability, high optoelectronic properties and high dielectric constant.

[1] Centurion University of Technology and Management, Odisha, India.
* Corresponding Author- Santosh.satpathy@cutm.ac.in

A most promising and high-efficiency Perovskite Photovoltaic cell can be developed by systematically investigations and implementation.

Keywords: Perovskites; Sb based Halide; Germanium Halide; Bi based Halide; PV Cells;

1. Introduction

Recently,A Photovoltaic cell is a most dynamic and optimistic technology which fulfils the globally necessary demand for energy [1]. It is undoubtedly considered the most promising never-ending energy source that converts light into electrical energy directly through photovoltaic effects and photochemical reactions. In 1883, the first semiconductor/ metal junction photovoltaic cell was developed by Fritts considering germanium with very low efficiency (nearly 1%). Later, Pearson prepared the first crystalline silicon PV cell in US Bell Labs with a 4.5% efficiency of conversion in the year 1954. It was the beginning era for the development and application of PV cells [2].

Photovoltaic cells are categorized as three-generation cells according to their development stages.

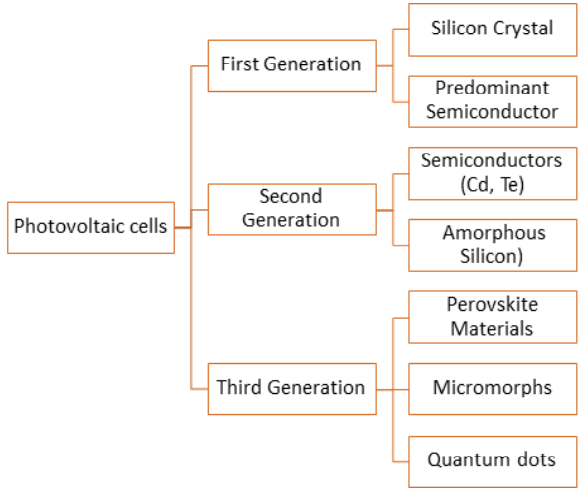

Since the 19th century, a large number of Photovoltaic cells were developed including silicon PV cells, Semiconductor PV cells etc., but Perovskite PV cells attracted much more attention from scientists and researchers due to the rapid improvement of the performance and efficiency of PV cells since 2006 [3]. The perovskite PV cells were invented in 2009 with better open-circuit voltage and 25% efficiency of power conversion. The characteristics of Perovskite such as high optical absorptivity[4], greater charge-carrier mobility, small carrier effective masses[5] photoelectric properties, high electronic dimensionality, longer exciton diffusion length, high optical absorption coefficients, easily tunable bandgap, low synthesize cost and low binding energy for excitation etc. make them suitable as photoactive material for photovoltaic cell[3]. Perovskite material with a high dielectric constant also can absorb solar energy adroitly [6]. Lastly, electrons and holes can be transmitted simultaneously up to 100 nm or more and even more than 1 5ØßmØ[2].

Although Lead halide-based perovskites show excellent behaviour for photovoltaics due to their unique properties such as narrow bandgap, the high value of absorption coefficient etc., the high toxicity, expensive transporting materials and poor stability behaviour of Lead prompted many scientists and researchers to develop lead-free perovskite Photovoltaic cells.

1. Lead-free Metal Halide Perovskite

Recently, less toxic metals such as Bismuth (Bi), Tin (Sn), Germanium (Ge) and Antimony (Sb) [7] and others having the same ionic radii and electronic configurations of Pb have been used in the place of toxic metal Lead (Pb) used for the preparation of Lead-free perovskite PV cells having good stability and performance [1]. The appropriate alternatives metal to lead should have the properties such as low toxicity, high stability, low manufacturing cost, high optoelectronic properties

and high dielectric constant etc. for the high conversion efficiency PV cell. Some favourable halide perovskites are Germanium based halide, Bi-based halide, Antimony based halide and tin-based halide etc. which are described below.

1.1. Germanium Halide Perovskite

Instead of Lead, we may employ Germanium in halide perovskite materials for photovoltaic applications. T. Krishnamoorthy prepared crystals MAGeI3 and FAGeI3 and observed that these crystals were suitable photovoltaic materials with photocurrent values of 5.7 and 4 mA cm^{-2} respectively[9]. Min Gang Ju predicted that RbSn0.5Ge0.5I3 is a promising material for Photovoltaic cells with a 0.9 -1.6 eV range of direct bandgap [10].

1.2. Bismuth halide-based perovskites

Bismuth as a nontoxic element may replace Lead for Photovoltaic material due to the same ionic radii and electronic configuration as Lead. The performance and efficiency of bismuth halide-based perovskite can be improved by the development of a charge extraction layer and doping of Bismuth based perovskite in future The synthesis of Bismuth halides-based perovskite was carried out for the application in Photovoltaics and the band gaps were observed to be in the range of 1.9 to 3.1 eV [7].

1.3. Antimony halide-based perovskites

Antimony having the same ionic radii, same structures as Bismuth and Lead may use in the place of toxic element Pb in the preparation of Photovoltaic cells. It also exhibits photo material properties such as high optoelectronic and high dielectric constant. The synthesis of Cs3Sb2I9 perovskite was demonstrated by computational and experimental processes [7]. It is observed that the efficiency and the

potential of Sb based photovoltaic cells can be developed by controlling phase transition and nucleation rate in future [11].

1.4. Tin based halide perovskites

The most promising environment-friendly element is tin for photovoltaic applications having large potential because of its same electronic configuration and ionic radius as lead (Pb2+:119 pm; Sn2+:110 pm). The first theoretical study on Tin perovskite PV cells with 5-6% efficiency of power conversion have been published in 2014, Stefan Weber demonstrated tin-based iodide perovskite and observed the increase of band gap value with an increase in the concentration of dopant [12]. The efficiency of the tin based photovoltaic cell can be increased by the use of a carboxylate antioxidant capping agent[13].

Conclusion

Further research should be focused on introducing new halide-based materials with suitable bandgaps and benign defects characteristics. A most promising and high-efficiency Perovskite Photovoltaic Cells can be developed by systematically investigations and implementation. Perovskite Photovoltaic cells can be the most efficient and promising future energy source with low cost, less/non-toxicity, high stability and high optoelectronic properties.

References

[1] K. Ahmad, (2020). *"Bismuth Halide Perovskites for Photovoltaic Applications,"* Bismuth - Fundam. Optoelectron. Appl.

[2] D. Zhou, T. Zhou, Y. Tian, X. Zhu, and Y. Tu, (2018). *"Perovskite-Based Solar Cells: Materials, Methods, and Future Perspectives,"* J. Nanomater., vol. 2018.

[3] M. I. H. Ansari, A. Qurashi, and M. K. Nazeeruddin, (2018). *"Frontiers, opportunities, and challenges in perovskite solar cells:A critical review,"* J. Photochem. Photobiol. C Photochem. Rev., vol. 35, pp. 1–24.

[4] J. Huang, Y. Yuan, Y. Shao, and Y. Yan, (2017). *"Understanding the physical properties of hybrid perovskites for photovoltaic applications,"* Nat. Rev. Mater., vol. 2,.

[5] Z. Xiao, W. Meng, J. Wang, D. B. Mitzi, and Y. Yan, (2017) *"Searching for promising new perovskite-bsed photovoltaic absorbers: The importance of electronic dimensionality,"* Mater. Horizons, vol. 4, no. 2, pp. 206–216.

[6] M. Moniruddin et al., (2018). *"Recent progress on perovskite materials in photovoltaic and water splitting applications,"* Mater. Today Energy, vol. 7, pp. 246–259,.

[7] Z. Jin, Z. Zhang, J. Xiu, H. Song, T. Gatti, and Z. He, (2020). *"A critical review on bismuth and antimony halide based perovskites and their derivatives for photovoltaic applications: Recent advances and challenges,"* J. Mater. Chem. A, vol. 8, no. 32, pp. 16166–16188.

[8] V. Pecunia, L. G. Occhipinti, A. Chakraborty, Y. Pan, and Y. Peng, (2020). *"Lead-free halide perovskite photovoltaics: Challenges, open questions, and opportunities,"* APL Mater., vol. 8, no. 10.

[9] T. Krishnamoorthy et al., (2015). *"Lead-free germanium iodide perovskite materials for photovoltaic applications,"* J. Mater. Chem. A, vol. 3, no. 47, pp. 23829–23832.

[10] M. G. Ju, J. Dai, L. Ma, and X. C. Zeng, (2017), *"Lead-Free Mixed Tin and Germanium Perovskites for Photovoltaic Application*," J. Am. Chem. Soc., vol. 139, no. 23, pp. 8038–8043.

[11] Y. Yang et al., (2020) *"Dimension-Controlled Growth of Antimony-Based Perovskite-like Halides for Lead-Free and Semitransparent Photovoltaics,"* ACS Appl. Mater. Interfaces, vol. 12, no. 14, pp. 1.062–17069.

[12] S. Weber, T. Rath, B. Kunert, R. Resel, T. Dimopoulos, and G. Trimmel, (2019), *"Dependence of material properties and photovoltaic performance of triple cation tin perovskites on the iodide to bromide ratio*," Monatshefte fur Chemie, vol. 150, no. 11, pp. 1921–1927,.

[13] M. Khan, (2015). *"Materials Chemistry A,"* J. Mater. Chem. A, no. 207890, p. 121.

Chitosan nanocomposites in dental application

Centurion Journal of
Multidisciplinary Research
ISSN: 2395 6216 (PRINT VERSION)
ISSN: 2395 6224 (ONLINE VERSION)
Centurion University of Technology
and Management
At - Ramchandrapur
P.O. - Jatni, Bhubaneswar
Dist: Khurda – 752050
Odisha, India

Himanshu B Samal[1], Nigam S Tripathy[2], Liza Sahoo[2] and Fahima Dilnawaz[2]

Abstract

Chitosan is a naturally occurring biopolymer that derived from deacetylation of chitin. Chitosan biomaterials have special qualities like biocompatibility, biodegradability, non-toxicity, muco-adhesion, and a broad spectrum of anti-bacterial, anti-fungal, antiprotozoal, anti-inflammatory, anticancer, antiplaque, anti-tartar etc. In addition, chitosan is the only cationic polysaccharide found in nature that can be chemically

[1] School of Pharmaceutical Sciences, Centurion University of Technology and Management, Jatni, Bhubaneswar-752020, India (Email; himansubhusan.samal@cutm.ac.in)

[2] Department of Biotechnology, School of Engineering and Technology, Centurion University of Technology and Management, Jatni, Bhubaneswar-752020, India (Email: fahima.dilnawaz@cutm.ac.in)

altered to create derivatives depending on the intended use and function. This review discusses chitosan's present, lucrative applications for the treatment of periodontitis and dentin-pulp regeneration, as well as its critical function in the creation of bio-dental materials.

Keywords: Nanocomposites, chitosan, biomaterials, dentistry, dental implant, metal oxides

Introduction

Recent years have seen tremendous advancements in the design and application of safe and useful materials thanks to the concept of biomaterials, which has been widely put forth (Fakhri E, 2020; Gao Y, 2022). Biological environments can be implanted with the use of biomaterials, which can be either all-natural, synthetic, or semi-synthetic materials (Chan, 2008; Sadreddini, 2017). Successful clinical applications of biomaterials can be found, primarily in reconstructive plastic surgery (Gosain AK, 2005), orthopaedic surgery (Cross *et al* 2016), cardiac surgery (Ozawa *et al* 2007), and dentistry (Zafar MS, 2019). These applications are primarily used to improve the organs or tissues functionality, as well as to restore their structural integrity. Enzymatically these biopolymers can be broken down into simpler forms that are neither toxic nor harmful to the environment. Additionally, depending on the field of use, they can be changed via chemical or enzymatic processes to other derivatives and different shapes including gels, micro/nanoparticles, fibres, sponges, and films (Qin, 2020).

Chitosan is a macromolecule created by the repeating of D-glucosamine, which is produced by the deacetylation of chitin found in the shells of marine crustaceans, particularly crabs and prawns. Chitosan, FDA-approved copolymer made of -(1 4) is chitosan.N-acetyl D-glucosamine and -2-acetamido-2-deoxy-b-D-glucan (1 + 4)-2-amino-2-deoxy-b-D-glucan (D-Glucosamine) units that are less crystalline and have a lower molecular weight than chitin (Husain S, 2017). Chitin and chitosan are

thus prospective ingredients for the production of a variety of dental materials, including scaffolds and drug carriers, due to their particular composition and multifaceted functioning (Husain S, 2017).

In acidic solvents with a pH lower than 6.0 chitosan is extremely soluble and insoluble in water and in nearly all organic solvents. This substance indicates higher solubility compared to chitin because free amino groups on the chitosan backbone are protonated in acidic solvents, which causes it to be polycationic (Bakshia PS & 2019; Husain S, 2017; Pillai C, 2009). When used in biomedical applications, this solubility is not preferred, especially at physiological pH levels of 7.4. The first step in broadening the applications of chitosan is to increase its solubility. There are practical ways to do this, including crosslinking, the chemical alteration of chitin through deacetylation, the enzymatic or chemical depolymerization or degradation of amino or hydroxyl groups, and the addition of hydrophilic biomolecules to these groups. According to several research, chitosan can be used in conjunction with synthetic and natural materials to create scaffolds with biomedical uses. Bioactive Nanoceramics such as ZrO2, TiO2, SiO2, and HAp, as well as different types of biopolymers, silk, and chitin have been added to chitosan-based biomaterials to improve their structural integrity and mechanical strength (Rahmani, 2018; Sharifianjazi, 2020; K. v. L. Zhang, Q., 2020). The aim of the current review is to examine chitosan compositions used during the past ten years in dental engineering and implanted scaffolds.

Nanocomposites of chitosan with carbon-based materials

Chitosan has a number of advantageous properties. Because of these characteristics, chitosan stands out as a biomaterial for a variety of uses. Composites are currently a key component of dentistry and implant materials, and have recently attracted lots of attention due to its biodegradability, biocompatibility, inherent antibacterial activity, having minimal interactions with a foreign body. Therefore, chitosan composites are proposed to be a potential material for artificial bone and bone

regeneration in the field of dentistry. Further, chitosan composite materials in the domains of dental and implant mode have recently attracted a lot of attention due to their varied geometries, porous structures (di Martino, 2005; Ladiè, 2021; Terada, 2009).

Carbon-based nanomaterials, such as graphene oxide (GO), graphene, and carbon nanotubes, are closely related due to their physical characteristics that resemble those of collagen fibres, a part of extracellular matrix components (Ku *et al* 2013). These carbon-based nanomaterials possess exceptional mechanical properties, that play a vital role in inorganic/organic/synthetic based scaffolds that are useful for applications in bone tissue engineering. Amiryaghoubi *et al.* in a recent study developed thermosensitive injectable hydrogel by employing chitosan as a natural polymer and various feed ratios via a copolymer/GO composite with both chemical and physical crosslinking based on poly (N-isopropyl acrylamide) (PNIPAAm). These hydrogels were employed to aid the human dental pulp stem cells (hDPSCs) to differentiate into osteoblasts and grow (Amiryaghoubi, 2020) . Titanium (Ti) has been a popular material for dental and bone surgical implants. The osseointegration of implants can be improved by titanium's surface modification. In a study, composite made of GO, chitosan, and hydroxyapatite (GO/CS/HA) was made on Ti substrates via electrophoretic deposition. Van der Waals bonding enables the connection between HA and GO. As a result, the GO, CS, and HA particles worked together to generate a more homogeneous coating for the GO/CS/HA-Ti. The surface wettability and hydrophilicity were also found to be better in GO/CS/HA-Ti. These qualities are linked towards maintaining uniform shape, smooth surface of it. The GO/CS/HA-Ti shown greater osseointegration during the *in vivo* animal study and had better bioactivity in terms of enhancing bone marrow stem cells (BMSC) cell adhesion, proliferation, and differentiation during *in vitro* cytological analysis. These findings imply that an alternate way for creating GO/CS/HA composite coatings on Ti implants is offered by

the electrophoretic deposition process. In the field of dental implant this type of coating may be used (Suo L, 2019). In a study, Javed *et al* (2020) formulated dental adhesives using CuO-Chitosan nanocomposites. Dental adhesive discs with CuO-chitosan nanoparticle reinforcement significantly increase the decrease of *Lactobacillus acidophillus* and *Streptococcus* mutans. Additionally, improvements in mechanical characteristics, better water absorption, solubility, slow sustained release profile, and a minor change in shear bond strength has been achieved. The synthesized CuO-NPs and CuO-Chitosan-NPs have remained as attractive candidates with great potentiality for drug delivery and nanotheranostics (Javed R, 2020).

Nano/composites of chitosan with polymer-based materials

Chitosan's hydrophilic properties are often reduced and its mechanical properties are increased by combining it with hydrophobic synthetic polymers. To design bone tissue synthetic polymers are utilized. The composition mixture of polylactide-co-glycolic acid (PLGA) and chitosan-NPs and microspheres are combined for local or systemic drug delivery for bioactive molecules. The chitosan-PLGA scaffold exhibited considerable osteogenesis and cellular compatibility compared to other PLGA-based composites. Constantin *et al* synthesized biocomposite films from poly(vinyl alcohol) (PVA) cross-linked with oxidized chitosan (OxCS), to which Ag-NPs were inserted during film synthesis. The film displayed a high swelling ratio, and suitable mechanical strength with mucoadhesive properties. The ibuprofen (IBF)-loaded composite film (IBF-loaded PVA/OxCS-Ag) could sustainably release the drugs. The formulation displayed better antimicrobial (*P. aeruginosa*, *P. gingivalis*, *S. aureus*, *K. pneumoniae)*, activity by demonstrating a high zone of inhibition. The anti-inflammatory activity for oral cavities is observed with more loading amount of silver in the composite films (Constantin M, 2022). The *in vitro* tests on (human dermal fibroblast adult) cells (HDFa) cell lines displayed that the films are biocompatible,

with suitable mechanical properties it can be applied to the periodontal pockets. The cytocompatibility of the pure and composite PVA/OxCS-Ag films, unloaded or loaded with IBF were assessed by conducting in *vitro* tests on HDFa cell line. The findings showed that the increased AgNPs content caused a reduction in cell viability. Cell viability dropped significantly with greater Ag levels, and the toxicity increased more after 48 hours of exposure (Constantin M, 2022).

The biomedical and healthcare industries stand to gain significantly from the use of three-dimensional (3D) printing, which is a cutting-edge manufacturing technique. 3D printing technology based on fused filament fabrication (FFF) technology, Singh *et al*. created chitosan-reinforced poly-lactic acid (PLA) scaffolds and tested their mechanical performances (tensile, compression, and flexural). Through the use of the design of experiments, it is specifically examined how the mechanical behavior of PLA composite scaffolds is affected by the loading of chitosan, the density of the infill, and the annealing temperature. Additionally, selective electron microscopy was utilized to study, the behaviour of fracture under various load types. It was found that the density of the infill and the loading of chitosan have a considerable impact on the strength of the composite samples, however, the temperature of annealing has no significant impact on its mechanical response. Overall, the created scaffold based on PLA composites are mechanically effective and seem to be appropriate for use in clinical settings (Singh, 2020).

Nanocomposites of chitosan with metal or metal oxides

Metal ions are important components of bone tissue. A few metal ions to mention are Zn2+, Cu2+, Mg2+, and Sr2+. Chitosan-metal composites are made using a variety of methods, including electrospinning, freeze-drying, sol-gel, and complexation interactions. The ability of chitosan to chelate with a variety of metal ions, particularly transition metal ions, is its most useful property. Additionally, metal oxides

like silica, zirconia, and alumina are frequently employed to improve the binding between restorative materials. Vaidhyanathan *et al.* used a freeze-dry technique to create a chitosan-silver composite scaffold. Thomas and colleagues used an in-situ method to create films of chitosan/silver nanoparticles. the photochemical reduction of silver ions in an acidic solution of chitosan and $AgNO_3$ (Thomas, 2009; Venkatesan, 2010).

Utilizing metallic nanoparticles and acid evaporation, zirconium oxide nanoceramic modified chitosan-based nanocomposite film was created (Bhowmick, 2017). To create bone-like nanocomposites for bone tissue engineering, zirconium oxide nanoparticles (ZrO2 NPs) were added to organic-inorganic hybrid composites including chitosan, poly(ethylene glycol), and nano-hydroxypatite (CS-PEG-HA). Addition of 0.1-0.3wt% of ZrO2 showed improved mechanical strengths and water absorption capacity when compared to CS-PEG-HA composite. The mechanical strengths and porosities were similar to spongy bone in humans. Strong antibacterial activities were also seen against gram-positive and gram-negative bacterial species. These nanocomposites in osteoblastic MG-63 cells displayed hemocompatibility and cytocompatibility in low alkalinity pH (7.4) values that are comparable to the pH of human plasma (Bhowmick, 2017).

As a bone implant, bare 316L stainless steel alloy (316L SS) was coated with nanocomposite coatings made of chitosan- NPs and cobalt (Co)-NPs. Co-NPs and chitosan-NPs were used in a fabrication of nanocomposite coatings for bone implants that were applied to bare 316L stainless steel alloy (316L SS). The comparison study between the monophasic coatings (CS-NPs & Co-NPs) and di-phasic coating (CoNPs-CSNPs), revealed that the di-phasic coating of (CoNPs-CSNPs) displayed higher electrochemical corrosion resistance with low hydrogen evolution rate. These corrosion findings indicated that a CoNPs-CSNPs nanocomposite coating on 316L SS was suitable for functional or renewable implants (Gawad SA, 2021). CoNPs were

produced, thereafter, bare 316L SS alloy was electrodeposited and covered with CSNPs. Furthermore, CNPs have proven to be antimicrobial against a variety of microorganisms. Additionally, adding chitosan to composites enhances their antibacterial properties without compromising their shear bond strength (SBS). Chitosan and gold (Au)-NPs based bio-nanocomposite were created using electrodeposition techniques. The influence of AuNPs/CS bio-nanocomposite film on the corrosion resistance of Ti was investigated. AuNPs/CS bio-nanocomposite is a good candidate for changing biomaterial surfaces for medical implantation applications because of the excellent biocompatibility of chitosan and the great adsorption capacity of AuNPs (Farghali, 2015).

Application of Chitosan Composites for Dentistry

Chitosan nanocomposites

Fluoride has been regarded as the most important and well-known dental agent. to avoid dental cavities. However, the significant prevalence of dental fluorosis raises some concern. Chitosan *in vitro* production of enamel demineralization inhibited by the discharge of mineral components from the enamel. The synergistic action of chitosan and propolis illustrated enhancing antibacterial activity. The chitosan composite based dentifrice significantly stopped enamel demineralization around the dental braces during orthodontic treatment. For pulp capping, the gypsum-based chitosan (Gp-CT) and calcium phosphate carboxymethyl-chitosan composite (CaP-CMCS) material can be used for the enhancement of human dental pulp stem cells, cytocompatibility, differentiation, and proliferation. It was determined that the compressive strength was greater than 600 kPa. This is more than calcium hydroxide, a typical pulp capping agent's compressive strength. Additionally, it was discovered that the swelling was less than 2% and the rate of disintegration was under 10%. Also noted was pulp stem cell odontoblastic differentiation. The CaP-CMCS composite has

odontogenic potential, is biologically compatible, has better mechanical qualities, and gels quickly. As a result, the CaP-CMCS composite exhibits biocompatibility, mechanical stability, and quick curing, which are the fundamental requirements of a candidate agent for pulp capping regeneration (Musat, 2021; C. H. Zhang, D.; Du, C.; Sun, H.; Peng, W.; Pu, X.; Li, Z.; Sun, J.; Zhou, C., 2021). The freeze-drying technique was used to create a porous chitosan/collagen scaffold, or chitosan/polymer-based composite. The surface of the synthetic scaffold was then seeded with human dental pulp stem cells (DPSCs)., that exhibited improved gene delivery and DPSCs differentiated to exhibit an odontoblast-like phenotype. Emulsion electrospinning was used by Shen *et al*. to create chitosan/PLA nanofibers. The performance and applicability of these nanofibers for periodontal bone regeneration were examined. The result demonstrated enhanced cell adherence and osteogenic differentiation of bone marrow stem cells (BMSCs). Also noted was the increase of TLR4 expression in human periodontal ligament cells (hPDLCs) (Shen, 2018; Yang, 2020). In a study, calcium hydroxide was combined with various mediums, including chitosan, calcium hydroxide, including distilled water, propylene glycol, and guttapercha points, to examine and quantify the change in pH and calcium ion release in the environment. The largest sustained release of calcium ions was seen in the chitosan formulation. It generated a high alkaline pH that lasted up to 30 days. Researchers discovered that self-assembly is a viable method for overcoming the limiting drug hydrophobicity on carrier structure formed by self-assembly of chitosan/phospholipid nanoparticles (SACPNs). SACPNs displayed high encapsulation efficiency of drugs, and extraordinary penetration into gastrointestinal and transdermal mucosa (Murugan, 2021).

Conclusion and future perspective

Since the organic component of bone implants is so crucial, their matrices are usually hybrid in their makeup. Synthetic polymers

outperformed natural polymers in trials on viability, mineralization, alkaline phosphate activity, and proliferation. Modification and synthesis of chitosan based different composites such as chitosan/metal/metal oxide-based, chitosan/polymer based, chitosan/carbon-based composites have illustrated favourable biomaterial that can be employed for dentistry, bone implants, and bone tissue engineering. Furthermore, despite of CNT's exceptional mechanical strength h and capacity to mimic natural bone function are depicting enough mechanical strength. Homogenous CNT dispersion in the chitosan matrix continues to be a challenge, For biomedical applications, CNTs must also be exceedingly pure, and it remained as a bottle neck to produce. Although chitosan composites have significant therapeutic and diagnostic potential in biological applications, but a dearth of substantial understanding for chitosan quality assessment could slow its uses across all application fields.

References

Amiryaghoubi, N. Pesyan, N.N; Fathi, M.; Omidi, Y. (2020). Injectable thermosensitive hybrid hydrogel containing graphene oxide and chitosan as dental pulp stem cells scaffold for bone tissue engineering. *Int. J. Biol. Macromol., 162*, 1338–1357. .

Bakshia PS, Selvakumara D, Kadirvelub K, Kumara N, & (2019). Chitosan as an environment friendly biomaterial–a review on recent modifications and applications, . *Int. J. Biol. Macromol., 150*, 1072–1083.

Bhowmick, A. Pramanik, N; Jana, P.; Mitra, T.; Gnanamani, A.; Das, M.; Kundu, P.P. . (2017). Development of bone-like zirconium oxide nanoceramic modified chitosan based porous nanocomposites for biomedical application. *Int. J. Biol. Macromol., 95*, 348–356.

Chan, B. K. Leong, K. (2008). Scaffolding in tissue engineering: general approaches and tissuespecific considerations, . *Eur. Spine J., 17*(4), 467–479.

Constantin M, Lupei M, Bucatariu SM, Pelin IM, Doroftei F, Ichim DL, Daraba OM, Fundueanu G. (2022). PVA/Chitosan Thin Films Containing Silver Nanoparticles and Ibuprofen for the Treatment of Periodontal Disease. . *Polymers (Basel). 15*(1), 4.

di Martino, A; Sittinger,.; Risbud, M.V. (2005). Chitosan: A versatile biopolymer for orthopaedic tissue-engineering. . *Biomaterials, 26*, 5983–5990.

Fakhri E, Eslami H, Maroufi P, Pakdel F, Taghizadeh S, Ganbarov K, Yousefi M, Tanomand A, Yousefi B, Mahmoudi S, Kafil HS. (2020). . Chitosan biomaterials application in dentistry. *Int J Biol Macromol., 162*, 956-974.

Farghali, R. Fekry,A.;Ahmed, R.A.; Elhakim, H. (2015). Corrosion resistance of Ti modified by chitosan–gold nanoparticles for orthopedic implantation. *Int. J. Biol. Macromol. , 79*, 787–799. .

Gao Y, Wu Y. (2022). Recent advances of chitosan-based nanoparticles for biomedical and biotechnological applications. *Int J Biol Macromol. , 203*, 379-388.

Gawad SA, Nasr A, Fekry AM, Filippov LO. (2021). Electrochemical and hydrogen evolution behaviour of a novel nano-cobalt/nano-chitosan composite coating on a surgical 316L stainless steel alloy as an implant. *International Journal of Hydrogen Energy, 46,*(35), 18233-18241.

Gosain AK, P.S.E.F.D. Committee (2005). Biomaterials for reconstruction of the cranial vault, . *Plast. Reconstr. Surg., 116*(2), 663–666.

Husain S, Al-Samadani KH., Najeeb S, Zafar MS, Khurshid Z, Zohaib S, Qasim SB. (2017). Chitosan biomaterials for current and potential dental applications. *Mater, 10*(6), 602.

Javed R, Rais F, Fatima H, Haq I ul, Kaleem M, Naz SS, Ao Q. . (2020). Chitosan encapsulated ZnO nanocomposites: Fabrication, characterization, and functionalization of bio-dental approaches. . *Materials Science and Engineering: C,, 116*, 11118.

Ladiè, R. Cosentino, C.; Tagliaro, I.; Antonini, C.; Bianchini, G.; Bertini, S. . (2021). Supramolecular Structuring of Hyaluronan-LactoseModified Chitosan Matrix: Towards High-Performance Biopolymers with Excellent Biodegradation. . *Biomolecules, 11*, 389.

Musat, V. Anghel, E.M ; Zaharia, A.; Atkinson, I.; Mocioiu, O.C.; Bu¸sila, M.; Alexandru, P. . (2021). A Chitosan–Agarose Polysaccharide-Based Hydrogel for Biomimetic Remineralization of Dental Enamel. . *Biomolecules, 11*, 1137.

Murugan, S. S. Anil., S.; Sivakumar, P.; Shim, M.S.; Venkatesan, J. (2021). 3D-Printed Chitosan Composites for Biomedical Applications. *In Chitosan for Biomaterials IV; Jayakumar, R., Prabaharan, M., Eds.; Advances in Polymer Science; Springer: Cham, Switzerland, 288*.

Pillai C, Paul W., Sharma CP. (2009). Chitin and chitosan polymers: chemistry, solubility and fiber formation,. *Prog. Polym. Sci., 34*(7), 641–678.

Qin, Y., Li, P (2020). Antimicrobial chitosan conjugates: current synthetic strategies and potential applications,. *Int. J. Mol. Sci., 21*(2), 499.

Rahmani, F. Moghadamnia, A.A..; Kazemi, S.; Shirzad, A. (2018). Motallebnejad, M. Effect of 0.5% Chitosan mouthwash on recurrent aphthous stomatitis: A randomized double-blind crossover clinical trial. . *Electron. Physician, 10*, 6912.

Sadreddini, S., Safaralizadeh R, Baradaran B, Aghebati-Maleki L, HosseinpourFeizi MA, Shanehbandi D, Jadidi-Niaragh F, Kafil

HS, V. Younesi, Yousefi M. (2017). Chitosan nanoparticles as a dual drug/siRNA delivery system for treatment of colorectal cancer, . *Immunol. Lett., 181*, 79–86.

Sharifianjazi, F. Pakseresht, A.H, Asl, M.S.; Esmaeilkhanian, A.; Jang, H.W.; Shokouhimehr, M. . (2020). Hydroxyapatite consolidated by zirconia: Applications for dental implant. *J. Compos. Compd., 2*, 26–34.

Shen, R. Xu, W.; Xue, Y.; Chen, L.; Ye, H.; Zhong, E.; Ye, Z.; Gao, J.; Yan, Y. . (2018). The use of chitosan/PLA nano-fibers by emulsion eletrospinning for periodontal tissue engineering. *Artif. Cells Nanomed. Biotechnol., 46*, 419–430.

Singh, S. Singh G.; Prakash, C.; Ramakrishna, S.; Lamberti, L.; Pruncu, C.I. (2020). 3D printed biodegradable composites: An insight into mechanical properties of PLA/chitosan scaffold. *Polym. Test. , 89*, 106722.

Suo L, Jiang N., Wang Y, Wang P, Chen J, Pei X, Wang J, Wan Q.T (2019). The enhancement of osseointegration using a graphene oxide/chitosan/hydroxyapatite composite coating on titanium fabricated by electrophoretic deposition. *J Biomed Mater Res B Appl Biomater., 107*(3), :635-645.

Terada, M. Abe, S.; Akasaka, T.; Uo, M.; Kitagawa, Y.; Watari, F. (2009). Development of a multiwalled carbon nanotube coated collagen dish. . *Dent. Mater. J., 28*, 82–88.

Thomas, V. Yallapu, M.M.; Sreedhar, B.; Bajpai, S (2009). Fabrication, characterization of chitosan/nanosilver film and its potential antibacterial application. . *J. Biomater. Sci. Polym.Ed, 20*, 2129–2144.

Venkatesan, J. Kim, S.-K. (2010). Chitosan composites for bone tissue engineering—An overview. . *Mar. Drugs, 8*, 2252–2266.

Yang, X. Han, G Pang, X.; Fan, M. (2020). Chitosan/collagen scaffold containing bone morphogenetic protein-7 DNA supports dental pulp stem cell differentiation in vitro and in vivo. *J. Biomed. Mater. Res. Part A, 108*, 2519–2526.

Zafar MS, Alnazzawi AA., Alrahabi M, Fareed MA, Najeeb S, Khurshid Z. (2019). Nanotechnology and nanomaterials in dentistry, . *Adv. Dent. Biomater.*, 477-505.

Zhang, C. Hui, D.; Du, C.; Sun, H.; Peng, W.; Pu, X.; Li, Z.; Sun, J.; Zhou, C. (2021). Preparation and application of chitosan biomaterials in dentistry. *Int. J. Biol. Macromol., 167*, 1198–1210.

Zhang, K. van Le, Q. (2020). Bioactive glass coated zirconia for dental implants: A review. . *J. Compos. Compd, 2*, 10–17.

Investigation of Antipshycotic Activity of Ethano Medicinal Plants of Cucurbitaceae Family

Centurion Journal of
Multidisciplinary Research
ISSN: 2395 6216 (PRINT VERSION)
ISSN: 2395 6224 (ONLINE VERSION)
Centurion University of Technology
and Management
At - Ramchandrapur
P.O. - Jatni, Bhubaneswar
Dist: Khurda – 752050
Odisha, India

Trayambica Acharya[1], Ashirbad Nanda[1*] and Rupali Rupasmita Rout[1]

Abstract

Psychosis is a frequent and severely handicapping symptom of many psychiatric, neurodevelopmental, neurologic, and medical diseases. Schizophrenia is a mental illness that results in abnormal behaviours, decreased affect, and altered thought and perception. The neurotransmitter most closely linked to the pathogenesis of psychotic illnesses is dopamine. Dopamine overproduction in the mesolimbic tract is thought to be the root cause of the positive symptoms of psychotic

[1] 1School of Pharmacy and Life Science, Centurion University of Technology and Management, Bhubaneswar-752050, Odisha, India

[*] Correspondence author's E-mail: ashirbadnanda@gmail.com, Contact no: +919777533626

disorders. Additionally involved is glutamate, an excitatory neurotransmitter. The leguminous plant Mucuna pruriens (MP), which thrives in all tropical regions and contains levodopa, was looked into as a possible levodopa substitution for Parkinson's disease sufferers. Polyphenols found in herbal drugs contribute to this regulation of depression. Clinical studies suggest that proinflammatory cytokines, which are present in polyphenols, may contribute to the pathophysiology of depression. According to a phytochemical examination of numerous secondary metabolites, phyto components include alkaloids, flavonoids, steroids, tannins, saponins, anthraquinone, terpenoids, and cardiac glycosides are present.

Keywords*: Psychosis, Anti depressant, Herbal drugs, Chemical constituents*

Introduction

A common and severely debilitating symptom is psychiatric, neurodevelopmental, neurologic, and medical conditions, psychosis is also a crucial area for investigation and treatment in neurologic and psychiatric practie.(1).A mental condition called schizophrenia causes behavioural disturbances, diminished affect, and abnormalities in thought and perception. It is characterized by the presence of negative symptoms, such as hallucinations, delusions, and disordered speech and behaviour (2). During a psychotic episode, a person may also have delusions. The most common sorts of delusions are as follows: Reliable Source: Erotomanic delusions: the conviction that someone else is in love with them. A strong conviction that one has great power or authority is known as having delusions of grandeur: the idea that someone can broadcast their thoughts for others to see (3). Postpartum psychosis is a mental emergency that could seriously harm mothers', infants', and families' health and well-being. Mania or a mixed-mood episode is the hallmark of PPP, but severe confusion, depression, and anxiety are also frequent (4) The neurotransmitter dopamine is most firmly inextricably

bound up with the pathophysiology of psychotic diseases. Positive symptoms of psychotic diseases are hypothesised to be caused by an excess of dopamine in the mesolimbic tract. Excitatory neurotransmitter glutamate is also involved. Several investigations have discovered a reduction in the N-methyl-D-aspartate (NMDA) glutamate receptor activity, which is the primary contributor to psychosis (5) .

Herbal approach for mitigation of phycosis

Levodopa-containing leguminous plant Mucuna pruriens (MP), which grows in all tropical climates, was investigated as a potential substitute for levodopa for people with Parkinson's disease. Mucuna pruriens has DDCI-like substances which is used to treat Parkinson's disease(6).

Ma Huang has only ever been linked to one case of mania, whereas ephedrine has been linked to cases of psychosis. Researchers looked into how clozapine and herbal medications including Fructus Schisandrae, Radix Rehmanniae, Radix Bupleuri, and Fructus Gardeniae interact with one another in schizophrenia patients.

Rhodiola rosea(roseroot) and Crocus sativus (saffron) for depression; Passiflora incarnata (passionflower), Scutellaria lateriflora (scullcap) and Zizyphus jujuba (sour date) for anxiety disorders; and Piper methysticum (kava) for phobic, panic and obsessive-compulsive disorder(7) Crocus sativus (Saffron) has been used to treat depression, with four RCTs currently existing supporting this use. One of the most promising plant treatments for the treatment of depression is rhodiola rosea, an adaptogen that is stimulating and may have antidepressant benefits (8).

Lavandula angustifolia's antidepressant effectiveness has been examined which has a lengthy history of usage in the treatment of nervous system problems (9)

The principal psychoactive action of cannabis, the most popular illegal drug, is caused by delta-9-tetrahydrocannabinol (9-THC) antagonising cannabinoid receptor type 1 (CB1)(10)

Guduchi (Tinospora cordifolia) SD causes anxiety, cognitive dysfunctions, and muscle control impairment in certain persons. Kapikachhu contains natural Levodopa (LD) and is free of drug-induced dyskinesias. The results reveal that MP extract decreased MPTPinduced neuroinflammation and reversed biochemical and behavioural deficits in PD mice, supporting its traditional use(11)

Glyccrhiza improved motor deficits and cognitive problems in rats with postischemia and middle cerebral artery blockage by suppressing microglia activation and proinflammatory cytokine production(12)

Shankhapushpi the extract inhibited scopolamine neurotoxicity, demonstrating neuroprotective effects. CP treatment reduced scopolamine's neurotoxic effects, indicating it is neuroprotective(13).

In post-mortem Alzheimer's brain tissue, curcumin binds to fibrillar Aß plaques and CAA in its isoforms, conjugates, and bio-available forms (14).

Borage's Echium amoenum. Traditional Persian medicine use the herb boreage as a thymoleptic and anxiolytic. The ability of borage to lessen stress and despair was examined using an RCT (15)

Since antiquity, depression-related illnesses have been treated with Banxia houpu, a TCM formula made up of Pinellia ternata, Poria cocos, Magnolia officinalis, Perilla frutescens, and Zingiber officinale. Banxia houpu decoction reduced blood triglyceride levels and increased the activation of natural killer cells in the spleen in rats subjected to a range of mild stresses for an extended length of time in an animal model of depression(16)

Phytopharmaceuticals as depressants

The anti-inflammatory compound willow bark (WB) was used to treat fever and pain. These substances contains prodrugs such as salicin that are converted to salicylic acid, the active substance, in the liver and gastrointestinal tract by salicylic alcohol. Cyclooxygenases (COX) are known to be inhibited by salicylic acid. Moreover, it has been demonstrated that WB can influence important cytokines that promote and inhibit inflammation, including TNF, IL-6, IL-1, IL-10, and IL-8. IL-6, IL-1, IL-10, IL-8, TNF, and IL-1 which are few examples of important pro- and anti-inflammatory cytokines that WB can modify. In addition to salicyl alcohol derivatives, WB's conatins polyphenols which play a part in this depression modulation. Clinical studies suggest that proinflammatory cytokines, which are present in polyphenols, may contribute to the pathophysiology of depression (17) .

Length of immobilisation (desperation) times when the test animals don't want to swim are indicative of the stress which induces a depressive condition. Antidepressant medications, regardless of their composition or mode of action, promote increased activity and shorten periods of immobility(18)

The phenylpropanoid triandrin and schizandra chinensis and Echinacea purpurea tinctures had the strongest antidepressant effects in the clofelin-induced depression test. The administration of rosavin increased the stimulating activity of L-DOPA as did the tinctures of Schizandra chinensis and Echinacea purpurea (19)

The rats developed a depressive condition after receiving L-DOPA treatment. This condition was distinguished by the rodents' dejected demeanour, severe hypothermia, and reduced locomotor activity. The impact was particularly pronounced in the extract of Eleutherococcus senticosus, syringin (III), and rosavin (I), which lowered the immobilisation period.

The aerial parts of the plant Polygonum viscosum include four sesquiterpenes: viscosumic acid, viscozulenic acid, viscoazucine, and viscoazulone, as well as a flavonoid glycoside shown to have CNS depressive properties. Movement gradually slowed down, which was indicative of the strong CNS depressive effect of viscoazucine and viscoazulone. Following administration of these substances, there was a gradual decrease in movement, which indicated mild CNS depressing action(20)

Several herbal extracts, including those from Curcuma longa, Withania somnifera, Crocus sativum, Centella asiatica, and Bacopa monniera, which contain high levels of flavonoids and antioxidant components, in a number of experimental rodent models have been demonstrated to have antidepressant effects (21).

A pentacyclic triterpenoid saponin with anti-depressive effects, wound-healing, antiulcer, and anti-hepatofibrotic activities, asiaticoside also has these properties. Because of the reduced oxidative stress, it helped with diabetic patients' cognitive impairment(22)

Mandukparniin is another name for C. asiatica, a plant whose leaves and preparations are believed to enhance memory. C. asiatica, sometimes referred to as "Brahmi" in traditional Ayurveda, is a plant with special medicinal characteristics. Besides used as a brain tonic, it is also used to treat rheumatism, elephantiasis, and skin conditions. Moreover, it preserves nerve cells, enhances memory, lessens pain, and prevents the death of neural cells(23)

Peganum harmala (family Zygophyllaceae) and Lepidium meyenii (family Brassicaceae) (maca) are examples of plants with potential CNS effects and antidepressant qualities. L. meyenii is utilised as a nutritional supplement and dietary energizer to enhance both physical and mental health.

Human MAO-A was suppressed by H. perforatum flower extracts have the highest levels of inhibition. Plant extracts were investigated by HPLC-DAD-MS and found to include favonoids, pseudohypericin, hypericin, hyperforin, adhyperforin, and hyperforin. The herb H. perforatum is frequently used to treat mild to moderate depression.

Chemical constituents of cucurbitaceae family

The non-nutritive chemical components of plants are known as phytochemicals and are those that exist naturally in them or are compounds that are generated from plants. Numerous phytochemicals, such as tannins, cardiac glycosides, terpenoides, polysaccharides, resins, saponins, carotenoids, and phytosterols are confirmed to exist by research on the cucurbitaceae family. Alkaloids, flavonoids, and phenolic compounds are the most important of these bioactive components of plants(24)

Traditional herbal treatments for a variety of ailments in Cucurbitaceae family. They've shown anti-inflammatory, anticancer, hepatoprotective, cardiovascular, and immunoregulatory effects(25)

One of the biggest genera in the Cucurbitaceae family is Trichosanthes. as well as in conventional drugs to treat a variety of human ailments. It is enhanced with a variety of phytochemicals and biologically active substances. Steroids, triterpenoids, and flavonoids are this plant genus's main chemical components(26)

A nutrient-rich plant with a wide variety of medicinal compounds is Momordica charantia . Various parts of the plant posses different chemical constituents which are beneficial(27)

Alkaloids, gentilic acid, guanylate cyclase inhibitors, gypsogenin, hydroxytryptamines, karounidiols, lanosterol, lauric acid, linoleic acid, linolenic acid, momordenol, momordicillin, momordicinin, momordicicosides, and momordin are among the chemical components

of momordica charantia, momordol, multiflorenol, myristic acid, nerolidol, oleanolic acid, oleic acid, oxalic acid, pentadecans, peptides, petroselinic acid, polypeptides, proteins, ribosome-inactivating proteins, rosmarinic acid, rubixanthin, spinasterol, steroidal glycosides, stigmastadiols, stigmasterol, ascorbigen, bsistosterol-d-glucicide, citruline, elasterol, flavochrome, lutein, lycopene, pipecolic acid, glutamic acid, thscinne, alanine, g-amino butyric acid, and pipecolic acid.(28)

Alkaloids, reducing sugars, resins, phenolic compounds, fixed oils, glycosides, saponins, and free acids are all present in fruits. Due to its special combination of qualities, Karela is a wonder medication for ailments(29)

Bryonia plan leaves contained alkaloids, flavonoids, steroids, tannins, saponins, anthraquinone, terpenoids, and cardiac glycosides, according to a phytochemical analysis of several secondary metabolites. Alkaloids, flavonoids, anthraquinoin, sterols, and terpenoids are all present in the plant Bryonia. Vitamin B like thiamine (vitamin B1), riboflavin (vitamin B2), niacin (vitamin B3), vitamin B6 (vitamin B7), and folate (vitamin B9) are abundant in fruits and leaves(30)

17 substances were isolated as a result of the current phytochemical study on T. kirilowii, including triterpenes, sterols, flavonoids, saccharide derivatives, alkaloids, and norsesquiterpenes. The first pyroglutamac acid was discovered in T. kirilowii(31)

Procyanidin B2, B3, procyanidin B9, kaempferol, and quercetin are all antioxidants derivatives and only a few of the phytoconstituents found in Cydonia oblonga. The Cydonia oblonga seed includes Citric acid, oxalic acid, and fumaric acid are examples of organic acids, as well as fat-soluble compounds like -tocopherol, -tocopherol, -tocopherol stigmastrol, sitosterol, and vitamin C. Tyrosine, Tryptophan, Tylenol, Valine, Proline, Hydroxypyroline, Aspartic Acids, and Asparagines are only a few of the free amino acids that are abundant in the seed. Additionally,

it contains phenolic components such as rutinoside, kaempferol, stellarin, lucenin, and vicenin(32).

4. Conclusion

Following a thorough review of the literature, we discovered that the plants amazing medical characteristics of the Cucurbitaceae family include anti-HIV, anxiolytic, antipyretic, anti-diarrheal, carminative, antioxidant, antidiabetic, antibacterial, laxative, anthelmintic, antitubercular, purgative, and hepatoprotective effects.. Some cucurbits' seeds or fruit portions are said to have purgative, emetic, and anthelmintic qualities because of the presence of the secondary metabolite cucurbitacin. This group's compounds have been investigated for their effects on the heart, cytotoxicity, hepatoprotection, and inflammation. Future research should focus on isolating and purifying these compounds to determine their precise mode of action and evaluate their safety and efficacy. Further exploration of these plants and their bioactive constituents may contribute to the discovery of effective and safe antipsychotic drugs, providing alternative treatment options for individuals suffering from mental health conditions.

Conflict of Interest

Author's declare no conflict of interest.

Acknowledgement

The authors thankful to the Board of Management School of Pharmacy and Life Sciences, Centurion University, Bhubaneswar, Odisha, for providing a suitable-scientific environment to write this review article.

References

1. Arciniegas, D. B. (n.d.). *Psychosis*. www.ContinuumJournal.com
2. Palaniyappan, L., Maayan, N., Bergman, H., Davenport, C., Adams, C. E., & Soares-Weiser, K. (2015). Voxel-based morphometry

for separation of schizophrenia from other types of psychosis in first episode psychosis. In *Cochrane Database of Systematic Reviews* (Vol. 2015, Issue 8). John Wiley and Sons Ltd. https://doi.org/10.1002/14651858.CD011021.pub2

3. March, D., Hatch, S. L., Morgan, C., Kirkbride, J. B., Bresnahan, M., Fearon, P., & Susser, E. (2008). Psychosis and place. In *Epidemiologic Reviews* (Vol. 30, Issue 1, pp. 84–100). https://doi.org/10.1093/epirev/mxn006

4. Friedman, S. H., Reed, E., & Ross, N. E. (2023). Postpartum Psychosis. In *Current Psychiatry Reports* (Vol. 25, Issue 2, pp. 65–72). Springer. https://doi.org/10.1007/s11920-022-01406-4

5. Perez Gutierrez, R. M. (2016). Review of Cucurbita pepo (Pumpkin) its Phytochemistry and Pharmacology. *Medicinal Chemistry*, *6*(1). https://doi.org/10.4172/2161-0444.1000316

6. Schizophr, C., Psychoses, R., Dubey, A., Ghosh, N. S., Agnihotri, N., Kumar, A., Pandey, M., & Nishad, S. (n.d.). *Hybrid Open Access Review Article Clinical Schizophrenia & Related Psychoses Herbs Derived Bioactive Compounds and their Potential for the Treatment of Neurological Disorders*. https://doi.org/10.3371/CSRP.DANG.081922

7. Kelly GS. (2001). Rhodiola rosea: a possible plant adaptogen. Altern Med Rev 6: 293–302

8. Akhondzadeh S, Tahmacebi-Pour N, Noorbala AA et al. (2005). Crocus sativus L. in the treatment of mild to moderate depression: a double-blind, randomized and placebo-controlled trial. Phytother Res

9. Felter HW, Lloyd JU. 2006 (1898). King's American Dispensatory. http://www.ibiblio.org/herbmed/eclectic/kings/main.html.

10. Erik W. Gunderson MD, Heather M. Haughey PhD, Nassima Ait-Daoud MD, Amruta S. Joshi MS, Carl L. Hart PhD

11. Dhama, K., Sachan, S., Khandia, R., Munjal, A., Iqbal, H. M. N., Latheef, S. K., Karthik, K., Samad, H. A., Tiwari, R., & Dadar, M. (2017). Medicinal and Beneficial Health Applications of Tinospora cordifolia (Guduchi): A Miraculous Herb Countering Various Diseases/Disorders and its Immunomodulatory Effects. *Recent Patents on Endocrine, Metabolic & Immune Drug Discovery*, *10*(2), 96–111. https://doi.org/10.2174/1872214811666170301105101

12. Chakravarthi, K.K., Avadhani, R., (2013). Beneficial effect of aqueous root extract of Glycyrrhiza glabra on learning and memory using different behavioral models: an experimental study. J. Nat. Sci. Biol. Med. 4, 420–425.

13. Kim Thu, Dang, Vui, Dao Thi, Ngoc Huyen, Nguyen Thi, Duyen, Duong Ky and Thanh Tung, Bui. (2020). "The use of *Huperzia* species for the treatment of Alzheimer's disease" *Journal of Basic and Clinical Physiology and Pharmacology*, vol. 31, no. 3, pp. 20190159

14. He, X.J., Uchida, K., Megumi, C., Tsuge, N., Nakayama, H., (2015). Dietary curcumin supplementation attenuates 1-methyl-4-phenyl-1,2,3,6-tetrahydropyridine (MPTP) neurotoxicity in C57BL mice. J. Toxicol. Pathol. 28, 197–206

15. Sayyah M, Sayyah M, Kamalinejad M. (2006). A preliminary randomized double blind clinical trial on the efficacy of aqueous extract of Echium amoenum in the treatment of mild to moderate major depression. Prog Neuropsychopharmacol Biol Psychia

16. Luo L, Nong Wang J, Kong LD, Jiang QG, Tan RX. (2000). Antidepressant effects of Banxia Houpu decoction, a traditional Chinese medicinal empirical formula. J Ethnopharmacol

17. Ulrich-Merzenich, G., Kelber, O., Koptina, A., Freischmidt, A., Heilmann, J., Müller, J., Zeitler, H., Seidel, M. F., Ludwig, M., Heinrich, E. U., & Winterhoff, H. (2012). Novel neurological and immunological targets for salicylate-based phytopharmaceuticals and for the anti-depressant imipramine. *Phytomedicine*, *19*(10), 930–939. https://doi.org/10.1016/j.phymed.2012.05.004

18. Annu, Baboota, S., & Ali, J. (2021). Combination antipsychotics therapy for schizophrenia and related psychotic disorders interventions: Emergence to nanotechnology and herbal drugs. In *Journal of Drug Delivery Science and Technology* (Vol. 61). Editions de Sante. https://doi.org/10.1016/j.jddst.2020.102272

19. Kurkin, V. A., Dubishchev, A. v, Ezhkov, V. N., Titova, I. N., & Avdeeva, E. v. (2006). MEDICINAL PLANTS ANTIDEPRESSANT ACTIVITY OF SOME PHYTOPHARMACEUTICALS AND PHENYLPROPANOIDS. In *Pharmaceutical Chemistry Journal* (Vol. 40, Issue 11

20. Datta, B. K., Datta, S. K., Chowdhury, M. M., Khan, T. H., Kundu, J. K., Rashid, M. A., Nahar, L., Sarker, S. D., & Sarker, S. D. (n.d.). *Analgesic, antiinflammatory and CNS depressant activities of sesquiter-penes and a flavonoid glycoside from Polygonum viscosum*.

21. Kumar, A., Konar, A., Garg, S., Kaul, S. C., & Wadhwa, R. (2021). Experimental evidence and mechanism of action of some popular neuro-nutraceutical herbs. *Neurochemistry International*, *149*. https://doi.org/10.1016/j.neuint.2021.105124

22. 1Jubilant Generics Limited, (Formerly Jubilant Life Sciences Division), D-12, Sector 59, Noida 201301, Uttar Pradesh, India

23. Nisha K, Sheel R, Kumar J. (2015). Tissue damage induces in vivo production of asiaticoside in Centella asiatica (Linn.) Urban. Int J Sci Res; 4(4): 2943-5

24. Rajasree, R. S., Francis, F., & William, H. (2016). Phytochemicals of Cucurbitaceae Family-A Review. *Available Online on Www.Ijppr.Com International Journal of Pharmacognosy and Phytochemical Research*, *8*(1)

25. Perez Gutierrez, R. M. (2016). Review of Cucurbita pepo (Pumpkin) its Phytochemistry and Pharmacology. *Medicinal Chemistry*, *6*(1). https://doi.org/10.4172/2161-0444.1000316

26. Pabuprapap, W., & Suksamrarn, A. (2021). Chemical constituents of the genus Trichosanthes (Cucurbitaceae) and their biological activities:A review. In *ScienceAsia* (Vol. 47, Issue S1, pp. 1–13). Science Society of Thailand under Royal Patronage. https://doi.org/10.2306/SCIENCEASIA1513-1874.2021.S012

27. Tanwar, S., Dhakad, P., Dhingra, G., & Tanwar, K. (2022). A review on salient pharmacological features and chemical constituents of bitter melon. *Biological Sciences*, *02*(02). https://doi.org/10.55006/biolsciences.2022.2207

28. Braca A, Siciliano T, D'Arrigo M, Germanò MP. Chemical composition and antimicrobial activity of Momordica charantia seed essential oil. Fitoterapia. 2008 Feb 1;79(2):123-5

29. Xu B, Li Z, Zeng T, Zhan J, Wang S, Ho CT, Li S. Bioactives of Momordica charantia as Potential Anti-Diabetic/Hypoglycemic Agents. Molecules. 2022 Mar 28;27(7):2175

30. Jawad, E., & Kadhim, E. J. (2019). *PHYTOCHEMICALS INVESTIGATION AND HEPATO-PROTECTIVE STUDIES OF IRAQI BRYONIA DIOICA (FAMILY CUCURBITACEAE) Antiproliferative activities of Althaea ludwigii L. extract on Michigan Cancer Foundation-7 breast cancer cell line View project PHYTOCHEMICALS INVESTIGATION AND HEPATO-PROTECTIVE STUDIES OF IRAQI BRYONIA DIOICA (FAMILY CUCURBITACEAE)*. https://www.researchgate.net/publication/338224535

31. Xu, Y., Chen, G., Lu, X., Li, Z. Q., Su, S. S., Zhou, C., & Pei, Y. H. (2012). Chemical constituents from Trichosanthes kirilowii Maxim. *Biochemical Systematics and Ecology*, *43*, 114–116. https://doi.org/10.1016/j.bse.2012.03.002

32. Din Ganaie, M. U., Behl, T., Nijhawan, P., Sachdeva, M., & Khan, N. (2020). Investigation of anti-depressant effect of aqueous and ethanolic extract of Cydonia oblonga in rats. *Obesity Medicine*, *18*. https://doi.org/10.1016/j.obmed.2020.100202

Thermodynamic properties of ternary liquid mixtures containing N-N dimethylformamide (DMF), Cyclohexane and Chloro-benzene at different frequencies

Centurion Journal of
Multidisciplinary Research
ISSN: 2395 6216 (PRINT VERSION)
ISSN: 2395 6224 (ONLINE VERSION)
Centurion University of Technology
and Management
At - Ramchandrapur
P.O. - Jatni, Bhubaneswar
Dist: Khurda – 752050
Odisha, India

Manoj Kumar Praharaj[1,*] and Subhraraj Panda[2]

Abstract

The Ultrasonic velocity, density and viscosity have been measured for ternary mixture of N-N dimethylformamide (DMF), Cyclohexane and Chloro-benzene at different frequencies (2 MHz, 4 MHz, 6 MHz and 8 MHz) for a constant temperature (318 K). These experimental data have been used to estimate the thermodynamic parameters such as adiabatic compressibility (â), free length (Lf), internal pressure (Ði), relaxation time (ô), acoustic impedance (Z), Gibb's free energy ("G) and absorption coefficient for the mixture.

[1] Ajay Binay Institute of Technology, Cuttack, Odisha-753014, India
[2] Centurion University of Technology and Management, Bhubaneswar, Odisha
[*] E-mail:, m_praharaj@rediffmail.com,subhrarajpanda@cutm.ac.in

Introduction

The practical importance of liquid mixture rather than single component liquid systems has gained much importance during the last two decades in assessing the nature of molecular interactions and investigating the physio-chemical behaviour of such systems [1,2]. Ultrasonic investigation of liquid mixtures consisting of polar and non-polar components is of considerable importance in understanding the physical nature and strength of molecular interaction in liquid mixtures. [3]. For a better understanding of the physio-chemical properties and the molecular interaction between the participating components of the mixtures, ultrasonic velocity together with density and viscosity are measured at different frequencies for different concentrations of the components in the mixture. These data furnish wealth of information about the interaction between ions, dipoles; hydrogen bonding, multi-polar and dispersive forces [4-5]. In order to understand the nature of molecular interactions between the components of liquid mixtures, it is of interest to discuss the same in terms of excess parameters rather than the actual values. The present paper deals with the study of different parameters of the mixture containing Dimethylformamide (DMF), Cyclohexane and chloro-benzene at different frequencies through ultrasonic measurements. DMF (C_3H_7NO) is a versatile compound. It is a non-aqueous solvent which has no hydrogen bonding in pure state. Therefore, it acts as an aprotic, protophilic medium with high dielectric constant and it is also considered as a dissociating solvent. DMF being a polar molecule results in dipolar and induced dipolar interaction between it and chlorobenzene in addition to dipolar-dipolar interaction between its molecules. DMF is primarily used as an industrial solvent. DMF solutions are used to process polymer fibres, films and surface coating to permit easy spinning of acrylic fibres to produce wire enamels and as a crystallization medium in the pharmaceutical industry. Cyclohexane (C_6H_{12}) is a non-polar, un-associated, inert hydrocarbon

possessing globular structure. It is produced in large quantity by hydrogenation of benzene. The principal use of cyclohexane is conversion by oxidation in air to a mixture of cyclohexanol and the ketone, which is then oxidized further to adipic acid for the manufacture of nylon. Cyclohexane belongs to alicyclic hydrocarbon (closed chain). The packing of carbon atoms in the even numbered alkane groups allows the maximum intermolecular attractions [6]. It is highly inert towards an electrophille or a nucleophille at ordinary temperature. Due to the non-polar nature of cyclohexane and its inertness towards electron donors[7], dispersive types of interaction are expected between it and other components. Chlorobenzene (C_6H_5Cl) is a poor electron donor towards the electron seeking proton of any group. It has low dielectric constant (å = 5.649) and dipole moment. (μ = 1.69 D). It is neither acidic nor basic and is more reactive because the chlorine atom is bonded with SP3 hybridised carbon atom and consequently can be removed easily. Hence the rate of reaction with chlorobenzene is faster. The rate of molecular interactions results in a greater degree of variation with respect to ultrasonic related parameters. The chlorine atom being an electron withdrawing atom attracts the À-electron of benzene ring in C_6H_5Cl and thus a decrease of the electron density of the ring takes place. This makes the benzene ring a relatively poor electron donor towards the Cyclohexane molecules. Hence a weak interaction between chlorobenzene and Cyclohexane is expected. In our system the dipole - induced dipole interaction between DMF and chlorobenzene is significant. Chlorobenzene is used as an intermediate in the production of commodities such as herbicides, dyestuffs and rubber. It is also used as a high-boiling solvent in many industrial applications as well as in the laboratory.

Experimental Section

The chemicals used in the present work were analytical reagent (AR) and spectroscopic reagent (SR) grades with minimum assay of 99.9%

were obtained from E-Merk Ltd (India). Various concentrations of the ternary liquid mixtures were prepared in terms of mole fraction, out of which the mole fraction of the second component Cyclohexane (X_2 = 0.4) was kept fixed while the mole fractions of remaining two (X_1 and X_3) were varied from 0.0 to 0.6. There is nothing significant in fixing the second component at 0.4.

(i) Velocity Measurement: - The velocity of ultrasonic waves in the ternary mixture has been measured using a multi-frequency ultrasonic interferometer with a high degree of accuracy operating at 11 different frequencies (Model M-84) supplied by M/s Mittal Enterprises, New Delhi. The measuring cell of the interferometer is a specially designed double-walled vessel with provision for temperature constancy. An electronically operated digital constant temperature bath (Model: SSI03spl) supplied by M/s Mittal Enterprises, New Delhi, operating in the temperature range -10o c to 85o c with an accuracy of ± 0.1K has been used to circulate water through the outer jacket of the double-walled measuring cell containing the experimental liquid.

(ii) Density Measurement: - The densities of the mixture were measured using a 25ml specific gravity bottle. The specific gravity bottle with the experimental mixture was immersed in a temperature-controlled water bath. The density was measured using the formula

$\tilde{n}_2 = (w_2/w_1).\ \tilde{n}_1$

where, w_1 = weight of distilled water, w_2 = Weight of experimental liquid,

$\tilde{n}_1$ = Density of water, $\tilde{n}_2$ = Density of experimental liquid.

(iii) Viscosity measurement: - The viscosities of the ternary mixture were measured using an Oswald's viscometer calibrated with double distilled water. The Oswald's viscometer with the experimental mixture

was immersed in a temperature-controlled water bath. The time of flow was measured using a digital racer stop watch with an accuracy of 0.1 sec.

The viscosity was determined using the relation,

$ç_2 = ç_1 (t_2/t_1) (ñ_2/ñ_1)$

Where, $ç_1$ = Viscosity of water, $ç_2$ = Viscosity of mixture,

$ñ_1$ = Density of water, ñ2 = Density of mixture,

t_1 = Time of flow of water, t_2 = Time of flow of the mixture.

Theoretical Aspect

The following thermodynamic parameters were calculated from Jacobson's relation [8–10].

(i) Adiabatic Compressibility (â):- Adiabatic compressibility is the fractional decrease of volume per unit increase of pressure, when no heat flows in or out. It is calculated from the speed of sound (U) and the density (ñ) of the medium by using the equation of Newton Laplace as,

$$â = 1/U^2.ñ \text{ ——— (1)}$$

(ii) Intermolecular free length (Lf) :- The intermolecular free length is the distance between the surfaces of the neighboring molecules. It is calculated by using the relation

$$L_f = K_T â^{1/2} \text{ ——— (2)}$$

Where, K_T is the temperature-dependent constant and 'â' is the adiabatic compressibility.

(iii) Free Volume (Vf) :- Free volume in terms of ultrasonic velocity(U) and the viscosity(ç) of liquid is

$$V_f = (M_{eff}.U/K.ç)^{3/2} \text{ ——— (3)}$$

Where 'M_{eff}' is the effective mass of the mixture, 'K' is a dimensionless constant independent of temperature and liquid. Its value is 4.281×10^9 .

(iv) Internal Pressure (Ði):- The measurement of internal pressure is important in the study of the thermodynamic properties of liquids. The internal pressure is the cohesive force, which is a resultant of force of attraction and force of repulsion between the molecules. It is calculated by using the relation,

$$Ïi = bRT\ (kç/U)\ 1/2\ (ñ^{2/3}/M^{7/6}) \text{ ——— (4)}$$

Where, 'b' stands for cubic packing, which is assumed to be '2' for all liquids, 'k' is a dimensionless constant independent of temperature and nature of liquids. Its value is 4.281×10^9 . 'T' is the absolute temperature in Kelvin, 'M' is the effective molecular weight, 'R' is the Universal gas constant.

(v) Relaxation time (ô):- Relaxation time is the time taken for the excitation energy to appear as translational energy and it depends on temperature and impurities. The relaxation time can be calculated from the relation,

$$ô = 4/3.\ (â.ç) \text{ ——— (5)}$$

Where, 'â' is the adiabatic compressibility and 'ç' is the viscosity of the mixture.

(vi) Acoustic impedance (Z):- The specific acoustic impedance is given by,

$Z = U.\tilde{n}$ ——— (6)

Where, 'U' and 'ñ' are velocity and density of the mixture.

(vii) Gibb's free energy:- The Gibb's free energy is calculated by using the relation

"G = kT.Ln (kTô/h) ——— (7)

Where, 'ô' is the viscous relaxation time, 'T' is the absolute temperature, 'k' is the Boltzmann's constant and 'h' is the Planck's constant.

(viii) Absorption coefficient:- Absorption coefficient or attenuation coefficient is a characteristic of the medium and it depends on the external condition like temperature, pressure, and frequency of measurement. It is given by the following relation [11].

$á = 8À^2 çf^2 / 3\tilde{n}U^2$ ——— (8)

Results and Discussion

The experimental data relating to density, viscosity and velocity at 318 K for frequencies 2MHz, 4 MHz, 6 MHz, 8 MHz for the mixture are given in table-I.

The intermolecular free length, as well as relaxation time, are properties of liquid mixtures which mainly affect the ultrasonic velocity. Intermolecular free length as well as relaxation time decrease with an increase in ultrasonic velocity. In the low-frequency range the molecules find greater time for interaction, for which they move with low velocities. When frequency increases, the molecules become less interacting with each other and move with larger velocities.

Since the association of the interacting molecules varies with the frequency of the ultrasonic wave, the cohesive force between the

molecules also varies. Cohesive force as well as internal pressure increases as frequency increases. Gibb's free energy increases with increase in frequency as well as mole fraction of DMF. The increasing value of Gibb's free energy suggests that the closer approach of unlike molecules is due to hydrogen bonding [12-13]. The increase in Gibb's free energy also suggests shorter time for rearrangement of the molecules in the mixture.

Attenuation coefficient which is a characteristic of the medium also increases with increase in frequency. This shows a similar behavior to that of the passage of electromagnetic waves through a conductor where the skin depth decreases with frequency of the incoming wave. Decrease in skin depth means increase in absorption. With increase in mole fraction of DMF, ultrasonic velocity, internal pressure, relaxation time and Gibb's free energy increases where as adiabatic compressibility, free length, free volume and acoustic impedance decreases. According to a model proposed by Eyring Kincaid [14], ultrasonic velocity should increase if the intermolecular free length decreases as a result of mixing of components. The decrease in adiabatic compressibility suggests that there is significant interaction between unlike molecules. The value of free volume decreases whereas internal pressure increases due to the various dispersive interactions and the columbic interaction existing between the component molecules. When an acoustic wave travels in a medium, there is a variation of pressure from particle to particle. The ratio of instantaneous pressure excess at any particle of the medium to the instantaneous velocity of that particle is known as "specific acoustic impedance" of the medium. This factor is governed by the inertial and elastic properties of the medium. In the present investigation acoustic impedance decreases with increase in concentration of DMF, Such a decreasing value of 'Z' further supports the possibility of molecular interaction between the unlike molecules. Viscous relaxation time and Gibb's free energy increases with increase in mole fraction of

DMF. The viscous relaxation time shows the presence of molecular interaction by addition of solvent concentration and the same is confirmed by Gibb's free energy parameter.

When frequency of the incoming waves is large, the response of the medium to the changes is relatively less. Hence it is observed that the acoustic parameters are highly affected at low frequency range as compared to the high frequency range. It may be concluded that in describing the thermal and acoustic parameters, the variation of the frequency plays a vital role. Further the non-linear variation of acoustical parameters with concentration reveals the complex formation.

References

[1] M. K. Praharaj, A. Satapathy, P. Mishra, S. Mishra, (2013). *Journal of Theoretical and Applied Physics,* 7(23).

[2] Manoj Kumar Praharaj & Sarmistha Mishra, (2018). *Journal of Therm. Anal. & Calorimetry*, 131(2), 1089-1094.

[3] Subhraraj Panda and Manoj Kumar Praharaj, (2022). *Indian Journal of Natural Sciences,* 13(71), 41274-41278.

[4] Biswajit Samantaray and Manoj Kumar Praharaj, (2022). *Indian Journal of Natural Sciences,* 13(71), 39581-39589.

[5] Manoj Kumar Praharaj, (2021). *"Journal of Scientific Research*," 13(1), 1-8.

[6] Manoj Kumar Praharaj and Subhraraj Panda, (2022). *"Indian Journal of Natural Sciences"*, 13 (71), 41720-41725.

[7] Manoj Kumar Praharaj and Subhraraj Panda, (2022). *"Indian Journal of Natural Sciences"*, 13(71), 41230-41235.

[8] S A Ikhe & M L Narwade, (2005). *Indian J Chem*., 44A, 1203.

[9] R Palani, S Sarvanan & A Geetha, (2007). *Asian J of Chem*., 19(7), 5113.

[10] R Thiyagarajan & L Palaniappan., (2008). *Indian J Pure & Appl. Phys*, 46, 852.

[11] M Aravinthraj, S Venkatesan and D.Meera, (2011). *J. Chem. Pharm*. Res., 3(2), 623-628.

[12] R J Fort , W R Moore, Trans Faraday, (1962). *Soc,* 61, 2102.

[13] A Ali, A K Nain, N Kumar & M Ibrahim, (2003). *Chin J Chem*, 21, 253.

[14] H Eyring, & J F Kincaud, (1938). *J. Chem Phys*, DOI: 10.1063/ 1.1750134, 6, 620-629

[15] S Thirumaran and S Sudha, (2010) *J. Chem. Pharm. Res*., 2(1), 327-337.

Table-1: Experimental Values of Density (ñ), Viscosity (ç) and velocity (U) at 2 MHz, 4 MHz, 6 MHz

and 8 MHz

Mole fraction		Density (ρ) $Kg.m^{-3}$	Viscosity ($\eta \times 10^{-3}$) $N.s.m^{-2}$	Velocity (U) $m.s^{-2}$			
X_1	X_3			2 MHz	4 MHz	6 MHz	8 MHz
0.0000	0.6000	975.254	0. 5486	1172.2	1169.2	1166.4	1165.9
0.0999	0.4999	959.400	0. 5509	1184.7	1181.6	1178.1	1176.9
0.1998	0.4001	942.248	0. 5536	1198.9	1194.6	1190.6	1188.1
0.3001	0.3000	923.528	0. 5573	1215.0	1209.6	1205.4	1202.0
0.4000	0.1999	903.075	0. 5594	1230.6	1224.4	1220.6	1216.0
0.4998	0.1001	880.712	0. 5615	1247.0	1241.8	1237.6	1233.0
0.5997	0.0000	855.982	0. 5631	1266.1	1261.6	1256.4	1251.5

Smart Ways of Biomaterial Designing:A Comprehensive Review

Centurion Journal of
Multidisciplinary Research
ISSN: 2395 6216 (PRINT VERSION)
ISSN: 2395 6224 (ONLINE VERSION)
Centurion University of Technology
and Management
At - Ramchandrapur
P.O. - Jatni, Bhubaneswar
Dist: Khurda – 752050
Odisha, India

Ashirbad Nanda[1], Rudra Narayan Sahoo[2], Bikash Ranjan Jena[1*], and Smruti Smaranika Sahoo[1]

Abstract

An interdisciplinary and highly intriguing area of research in academia and the biotechnology industry is the modification of human tissues to treat diseases. By interacting with human cells, three-dimensional (3D) biomaterial scaffolds can be extremely important in the morphogenesis

[1] School of Pharmacy and Life Science, Centurion University of Technology and Management, Bhubaneswar-751009, Odisha, India
[2] Department of Pharmaceutics, School of Pharmaceutical Sciences, Siksha O Anusandhan (Deemed to be University), Bhubaneswar, Odisha-751003, India.
[*] Corresponding author's E-mail: bikashranjan.jena@cutm.ac.in

of newly formed tissues. Both organic (from nature) and synthetic (man-made) materials have been used to create polymer-based biomaterials. Simple polymeric biomaterials can offer the mechanical and physical characteristics necessary for tissue development; nevertheless, the promotion of the production of functional tissues is still hampered by the absence of biomimetic qualities and interactions with human progenitor cells. Therefore, the next step in creating intelligent 3D biomimetic scaffolds that actively interact with human stem cells and progenitors while maintaining structural integrity to quickly build functional tissue could be the development of advanced functional biomaterials that respond to stimulation. The current review intensifies various types of biomaterials, its designing, method of preparations for synthesis and its biomedical applications, including the transport of bioactive chemicals and cell adhesion mediators as well as the fabrication of functional tissues to cure diseases, smart biomaterials preparations and its applications are deemed to be necessary to interact with the biological systems.

Keywords: Polymer, extracellular matrix, smart materials, tissue engineering, carbon dots, Ceramics, polymeric nanoparticles,

1. Introduction

After a sickness or an injury, the process of regaining function and helping the body's natural healing can be significantly aided by the use of biomaterials in today's medical practise. In the field of medicine, biomaterials are utilised either as a scaffolding for healthy tissue or as substitutes for biological elements that are not functioning well. Both naturally occurring and artificial biomaterials can be utilised. Sutures made of animal sinew were the first biomaterials ever used in medical practise, and they originated in ancient Egypt (Brovold, 2018; Vince et al., 1991; Nanda et al., 2021). The contemporary study of biomaterials draws inspiration from a wide variety of fields, such as medicine, biology,

physics, chemistry, tissue engineering, and materials science. In the past ten years, there have been significant advancements made in a variety of fields, including tissue engineering, regenerative medicine, and others, which have contributed to the field's explosive growth. Biomaterials can be made from a wide variety of different things, including metals, ceramics, polymers, glasses, and even biological cells and tissue. They can be recycled for use in healthcare in a variety of ways, including the production of moulded or machined parts, coatings, fibres, films, foams, and fabrics. Heart valves, artificial hips, dental implants, and even contact lenses are all examples (Bao et al., 2013; Megeed et al., 2002). A good number of them break down on their own over the course of time, while others can be absorbed by the body and then gently flushed out once they have completed their function. Metals, polymers, ceramics, and composites are just some of the biomaterials that can be discovered in nature or manufactured in the laboratory through a variety of different chemical processes. Other biomaterials include composites, which are made up of a combination of different materials. In many cases, biomedical equipment and living structures that are employed or adapted for medical purposes serve the same or similar activities as their natural equivalents, but they do so in a different manner (Sofia, Et al., 2001; Ferry, and Morrison, 1947).The heart valve is an example of a function that is considered to be more passive, while hydroxyapatite-coated hip implants are an example of a function that is considered to be more bioactive and serves a more interactive purpose. In the domains of dentistry, surgery, and drug delivery, biomaterials are also utilised on a consistent basis. For instance, the implantation of a construct into the body that contains impregnated pharmaceutical products can enable the prolonged release of a medication.This can be accomplished through the use of drug delivery systems. In addition to autografts, allografts, and xenografts, biomaterials also have the potential to serve as xenografts. xenografts are transplanted organs from a different species (Brovold, 2018; Vince et al., 1991; Nanda et al., 2021). It can be difficult to define

biomaterial; however, the following is one attempt at doing so: The term "biomaterial" refers to "any material, natural or synthetic, that comprises all or part of a living structure or biomedical device that performs, augments, or replaces a natural function." Biomaterials can be found in live organisms as well as biomedical devices. When applied within the context of medicine, the term "biomaterial" refers to any substance that has been modified for the purposes of therapeutic intervention (Ferry, and Morrison, 1947; Ghose, et al., 2023). A heart valve is an example of a biomaterial with a beneficial function, and hydroxy-apatite coated hip implants are an example of a biomaterial with an interactive function (the Furlong Hip, made by Joint Replacement Instrumentation Ltd. in Sheffield is an example of a bioactive biomaterial; such implants can last for more than twenty years). Another example of a biomaterial with both a beneficial and an interactive function is an artificial kidney. Another area that frequently makes use of biomaterials is the pharmaceutical industry, specifically drug delivery (where an implanted drug-impregnated construct can enable slow, continuous dosing) (Peng, et al., 2017).

2. Biomaterial and It's Types

Metals, polymers, ceramics, and composites can be extracted from the earth or synthesised in the laboratory through a variety of chemical processes, resulting in the use of biomaterials. They are frequently adapted for medical use and may consist of either the original material or biomedical technology designed to serve the same purpose as the original or to enhance it. Hip replacements with hydroxyapatite coatings are bioactive, whereas a heart valve is passive. In the disciplines of medicine, dentistry, and drug delivery, biomaterials are frequently employed. Using a construct impregnated with pharmacological components, for example, a drug can be steadily released into the body (Brovold, 2018; Ghose etal., 2023). Transplant materials, such as autografts, allografts, and xenografts, are another example of biomaterials.

In dentistry and medicine, biomaterials are substances that interact with cells and biological fluids. Most people's first encounter with biomaterials is through dental restorations, but they are increasingly relying on them for hip and knee replacements and cardiovascular repairs. Not only do these biomaterial implants improve the quality of life for the elderly with extended life expectancies, but they also assist an increasing number of younger individuals with cardiac disorders, traumas, or genetic disorders (Peng, et al., 2017; Jena, and Chakraborty 2021; Goswami, 2019)

Biomaterials play a crucial role in modern medicine by restoring function that has been lost as a result of illness or destruction. Biomaterials have numerous therapeutic applications including the maintenance, improvement, and replacement of biological tissue and functions. They can be either organic or man-made. The ancient Egyptians were the first people in history to utilise biomaterials; they created the first sutures out of animal sinew. Recent advances in tissue engineering and materials science have also had an impact on the field of biomaterials research. Due to breakthroughs in regenerative medicine, and other sectors. the field has grown rapidly during the past decade (Kim et al., 2017). Biomaterials can be made of anything from inanimate matter like metals and plastics to organic materials like live cells and tissue. Molded coatings, filaments, and textiles made from these materials can all be repurposed for use in healthcare. Contact lenses, dental implants, artificial hips, and artificial heart valves all fall within this category. Many of these medical aids break down naturally over time, and others can even be absorbed directly by the body (Goswami, 2019; Kim et al., 2017).

A **biomaterial** has been classified as the following properties:

a. It is a non-viable material or mixture. In other words, this stuff is incapable of evolving, expanding, or, to be honest, surviving.

b. This material might be solid or liquid, and it can be naturally or artificially generated.

c. The material is used to partially or completely replace, regenerate, repair, or augment any organ, tissue, or biological component in terms of shape and/or function.

d. The medicine is utilised to improve or maintain a person's quality of life.

e. The substance is not a narcotic (Kim et al., 2017; Li Z, et al., 2005; Griffith and Naughton, 2002).

2.1. Design of Biomaterials

A biomaterial is a material that is a non-viable substance meant to interact with living processes. The biomaterials' effective and reliable qualities allow them to be used in a physiological environment. These distinguishing features are provided by an appropriate Blend of physico-chemical and biological capabilities in order to develop well-known biomaterials. Polymers, metals, composites, and ceramics are used to create these biomaterials in a novel way. The vast majority of biomaterials on the market today were created either independently or in conjunction with elements from these classes (Kim et al., 2017; Li Z, et al., 2005; Griffith and Naughton, 2002). Each of these material classes has a unique atomic arrangement, resulting in a diverse set of structural, physical, chemical, and mechanical properties. As a result, these materials have a wide range of possible applications in the human body. The subsequent sections represent the material classifications (Naughton, 2002).

2.1.1. Polymers

Polymers are employed in cardiovascular devices to replace and promote the growth of various soft tissues, and they might be useful for biomedical applications. Patients have received implants made of various polymeric materials. The aforementioned substances are currently being employed in a wide variety of medical applications,

including but not limited to the following: heart valves, artificial hearts, vascular grafts, breast prostheses, dental materials, contact and intraocular lenses, fixtures for extracorporeal oxygenators, dialysis and plasmapheresis systems, coating materials for medical products, surgical materials, and tissue adhesives, just to mention just a few. The makeup, arrangement, and structure of the macromolecules that make up a polymer define its qualities. (Griffith, and Naughton, 2002). Additionally, the flexibility of several applications needs the creation of polymers with suitable physicochemical, interfacial, and biomimetic properties in order to perform certain activities. It is necessary to synthesise these polymers in a variety of forms and compositions. In comparison to other types of materials, polymeric biomaterials have a number of advantages, including (i) their relative ease of secondary processing, (ii) their availability with the required mechanical and physical properties, (iii) their availability, and (iv) their relative affordability. In the medical sector, polymers of both natural and synthetic origin are used. Acrylics, polyamides, polyesters, polyethylene, polysiloxanes, and polyurethane are just a few examples of synthetic polymeric systems. Synthetic polymers frequently lack biocompatibility, leading to the development of inflammatory reactions following the application of them. Natural polymers may hold the key to a solution. Natural polymers employed in biomedical applications include chitosan, carrageenan, and alginate (Kim et al., 2017; Li Z, et al., 2005; Griffith, and Naughton, 2002).

2.1.2. Metals

Metal-based implant materials have a rich tradition of providing vital therapeutic value in the medical profession. Heavy tungsten alloys include stainless steel (316L), titanium and its alloys (Cp-Ti, Ti6Al4V), cobalt chromium alloys (Co-Cr), aluminium alloys, zirconium niobium, and zirconium niobium. Metals and metal alloys have also been employed in the medical area. A small selection of the numerous metal-based medical products that have been made possible by the quick

development of biomaterials includes dental implants, craniofacial plates and screws, pieces of artificial hearts, pacemakers, clips, valves, balloon catheters, medical devices and equipment, bone fixation devices, dental materials, medical radiation shielding products, prosthetics, and orthodontic devices (Griffith, and Naughton, 2002; Kaushal et al 2001; Giri, et al., 2012). Although a wide variety of materials can be employed in the biomaterial's creation process, metals are often the material of choice for engineers. This is because metals can be easily shaped into the ideal biomaterial. Metals are often chosen for use in biomedical applications due to their low cost, high corrosion resistance, high mechanical strength, and excellent biocompatibility.

2.1.3. Carbon Dots

Diseases and dysfunctions of the skeletal system place significant strains on our ageing population. Preventative measures, such as the early diagnosis and treatment of bone-related disorders, can help alleviate this issue. To this end, researchers have maintained a focus on creating cutting-edge bone-specific imaging and drug delivery materials. However, there is a severe lack of materials with a high affinity and specificity for bone. Synthesised carbon dots (C-dots) from carbon nanopowder exhibit strong binding to calcified bone in vivo. In this study, we demonstrate the specificity and safety of bone binding to a class of C-dots. Notably, C-dots made from other sources lacked the bone-binding capabilities expected of them [9,10]. The heterogeneous nature of C-dots is highlighted by these variations, which are linked to changes in the surface chemistry of C-dot preparations. Importantly, chemical functionalization of the surface of C-dots generated from carbon nanopowder does not dramatically modify their bone-binding properties. Carbon nanopowder-derived C-dots have the potential to be used as extremely bone-specific bioimaging agents and medication carriers because to their distinctive characteristics (Peng, et al., 2017; Jena, and Chakraborty 2021).

The notion of carbon-based nanoparticles has lately gained considerable advances and established new breakthroughs in the areas of biological applications, tissue imaging, and cancer treatments such as breast cancer suppression. This was accomplished relatively recently. According to new scientific findings, the pharmacological agents and controlled drug delivery systems that are based on CBNs offer a wide variety of potential uses in a variety of different fields. On the other hand, the early identification, diagnosis, and management of tumour cells (breast cancer) are some of the most challenging applications of this technology (Peng, et al., 2017; Jena, and Chakraborty 2021). According to the research that has been conducted on the topic, numerous imaging modalities, such as magnetic resonance imaging (MRI) and ultrasonography, have been shown to be effective at detecting breast cancer in its earlier stages. Additional treatments are available for the eradication of cancer cells that have spread to the designated location, and some of these treatments include chemotherapy, radiation therapy, and sophisticated surgical procedures. On the other hand, recent studies and breakthroughs in the field of CBN have revealed an all-encompassing path to recovery for individuals who are afflicted with metastatic breast cancer. Carbon nanomaterials such as nanotubes, graphene, and fullerene are of interest to society as well as the scientific community for a variety of reasons, including their one-of-a-kind physicochemical and biological properties, the chemical composition agglomeration they exhibit, and the solubility characteristics they possess. It's possible that these characteristics have a greater impact on the biomolecules and cells of the target (Goswami, Bhat, and Patnaik, 2019).

2.1.4. Composite Materials

Composite engineering materials are made up of two or more physically and/or chemically separate constituent materials that are correctly arranged or distributed and have physical properties that differ from the constituent elements. The matrix is a continuous bulk phase in

composite materials, whereas the reinforcement is one or more discontinuous dispersion phases (Goswami, Bhat, and Patnaik, 2019). The reinforcement frequently outperforms the matrix in terms of quality. Aside from the matrix and reinforced phases, there is a third phase known as the interphase between the matrix and reinforced phases. Since composites have unique properties and are frequently stronger than the basic materials they are formed from, they are used to solve difficult problems when tissue in-growth is required. In recent years, the development of various biomedical composite materials has been the focus of scientific research because they offer novel alternatives to tissue load-bearing components. Composite scaffolds with porous structures made from blends of bio glass particles and biodegradable fibres are one example of this (Goswami, Bhat, and Patnaik, 2019; Kim et al., 2017). biomaterials offer an alternate option to improve several unfavourable characteristics of homogeneous materials (metals or ceramics), despite the fact that metals and ceramics have drawbacks including truncated biocompatibility and deterioration, as well as breakability and short rupture strength, respectively. A composite biomaterial's final composition is significantly influenced by the characteristics of the individual components. Linear expansion is a crucial factor to consider while creating composite biomaterials. When creating composites, it is usual practise to combine materials having comparable linear expansion constants. The goal of the implant may be defeated if the contact region (interface) between the reinforcement and matrix materials results in significant gaps via the contact surface due to different linear expansion constants between the component materials. Therefore, while choosing each component of the composite biomaterial, bone tissue engineers need to be more careful (Kim et al., 2017)

2.1.5. Ceramics

Another type of material used in the creation of biomaterials is ceramic. Because of its exceptional wear resistance, high compressive strength,

and inert body, ceramics were chosen. They were also chosen for their outstanding formability into a variety of shapes and porosities. Heart valves, biocompatibility coatings for metallic implants, artificial knees, hip prostheses, bone grafts, dental and orthopaedic implants, orbital and middle ear implants, and musculoskeletal system parts are all made of ceramic. Though less frequently than metals or polymers, ceramics are used in the manufacturing of biomaterials. Ceramics have a very limited range of applications due to their fragility and low tensile strength. Apatite had a significant influence in the creation of the pottery (Griffith, Naughton, 2002; Shivani, Jashandeep, Singh, 2021). Calcium phosphate-based biomaterials, which are used in a number of ways throughout the body, cover every skeletal component. Some of its uses include dental implants, transdermic devices, the treatment of fractures and bone anomalies, total joint replacement, orthopaedics, cranio-maxillofacial reconstruction, otolaryngology, and spinal surgery. Second, to rectify bone abnormalities, hydroxyapatite has been implanted in load-free anatomical locations including the middle ear and nasal septum. Additionally, bio-eye hydroxyapatite orbital implants and ceramic hydroxyapatite block implants are made with hydroxyapatite. In addition to these applications, hydroxyapatite has been used as a coating material for implants made of stainless steel, titanium, and its alloys, as well as metallic orthopaedic and dental implants, to aid in bone attachment (Goswami, Bhat, and Patnaik, 2019; Kim et al., 2017). In this case, the metal surfaces of the underlying bone structure are tightly adhered to by the hydroxyapatite. Contamination must be prevented at all costs, though. The failure of an implant and the significant difficulties it causes are the result of the ceramic layer delaminating from the metal surface.

Basic Considerations to Design Biomaterial

- While several devices and implants constructed from the aforementioned materials are being created to treat a wide range of medical conditions and injuries, the following fundamental concerns underpin the development of all biomaterials:

- Specifications according to which a biomaterial is developed. Accurately describing the biomaterial's intended environment and how that environment will influence the biomaterial's properties.

- Both the potential risks and benefits of using the biomaterial, as well as its expected lifespan, should be thoroughly understood before its implementation (Kaushal, et al., 2001; Giri et al., 2012).

3. Biomedical Applications

Implant materials made of metallic substances have a long history of playing an important therapeutic role in the field of medicine. Metals and metal alloys have been used in the medical field, including stainless steel (316L), titanium and its alloys (Cp-Ti, Ti6Al4V), cobalt chromium alloys (Co Cr), aluminium alloys, zirconium niobium, and tungsten heavy alloys. The rapid development of biomaterials has allowed for the creation of a wide variety of metal-based medical products including dental implants, craniofacial plates and screws, pieces of artificial hearts, pacemakers, clips, valves, balloon catheters, medical devices and equipment, bone fixation devices, dental materials, medical radiation shielding products, prosthetics, and orthodontic devices. Biomaterials can be made from a wide variety of various substances. engineers typically favour using metals as the primary material to construct the necessary biomaterial (Giri et al., 2012; Moran et al., 2014; Katari et al., 2014). This is due to the fact that metals can be easily manipulated to create the desired biomaterial. Because of their outstanding biocompatibility, practical mechanical qualities, great corrosion resistance, and low cost, materials based on metal are frequently selected for use in biomedical applications. When a metal-based biomaterial is introduced into a biological medium, the surface of the material may undergo changes and eventually degrade, resulting in the production of a number of different by products. This releasing process makes it possible for cells or tissues to interact with the surface of the metal device. Because of

this, current researchers are putting a lot of effort into learning about the surface properties of metals so they can make materials that are safe for living things (Wagner et al., 2013; Lee, Singla, Lee 2001; Ghose et al., 2021).

A detail description of Classification of materials used in therapeutic purposes, its advantages, and disadvantages have been elucidated in **Table 1**.

Table 1: Description of Biomaterials and its Merits and Demerits

Class of the Material	Merits	Shortcomings	References
Types of Polymers			
PTFE, silicones, Nylon,	Resilient Easy to fabricate	Not strong Deform with time, may degrade	(Ghose et al., 2021; Mckellop, Bradley, 1993; Edidin, Kurtz, 2000). Kumar et al., 2020); Dowson, Wallbridge, et al, 1985).
Metals		(Edidin, and Kurtz 2000; Kumar et al., 2020; Dowson, and Wallbridge, 1985; Radulovic, and Wojcinski 2014).	
Titanium, stainless steels, Co-Cr alloys, gold	Strong Tough, Ductile	May corrode High density	
Ceramics			
Aluminium oxide, Carbon dots. Hydroxyapatite	Highly biocompatible, Inert, high modulus Compressive strength Good esthetic properties	Brittle, Difficult to make, Poor fatigue resistance	(Radulovic, and Wojcinski. 2014; Shekhawat *et al*., 2021; Shivani et al., 2021; Hernigou, and Bouthors, 2016; Bernache-Assolant 1992; Hootman, et al. 2015)

4. Conclusion

In recent years, there has been a rise in interest in natural polymers based on proteins or polysaccharides because of the numerous applications that could be found for them in the field of biomedicine. These materials have a wide range of potential uses due to their chemical stability, structural plasticity, biocompatibility, and great availability. Some examples of these potential applications include tissue engineering, drug delivery, and wound healing. Biomaterials that were purified from animal or plant sources have also been engineered in order to improve their structural properties or promote interactions with the cells and tissues that surround them for improved in vivo performance. This has led to the development of novel applications such as implantable devices, controlled drug release, and surface coatings. This article provides a description of biomaterials that are generated from or inspired by natural proteins and polysaccharides and illustrates the promise that these biomaterials hold across a variety of different biomedical sectors. We provide an overview of the therapeutic applications that are now being made use of these naturally occurring materials, and we discuss the anticipated future developments in locating and making use of novel biomaterials in many new medical applications.

Funding

No Funding has been received in the current review work.

Conflict of Interest

Author's declare no conflict of interest.

Acknowledgement

The authors thankful to the Board of Management School of Pharmacy and Life Sciences, Centurion University, Bhubaneswar, Odisha, for providing a suitable-scientific environment to write this review article.

References

Bao, Ha T. L., Minh, T., Nguyen, D., & Minh, D. (2013). Naturally Derived Biomaterials: Preparation and Application. InTech. doi: 10.5772/55668. SofiaS Functionalized silk-based biomaterials for bone formation. *Journal of Biomedical Materials Research,* 200154139148.

Brovold, M., Almeida, J. I., Pla-Palacín, I., Sainz-Arnal, P., Sánchez-Romero, N., Rivas, J. J., & Baptista, P. M. (2018). Naturally-derived biomaterials for tissue engineering applications. *Novel biomaterials for regenerative medicine*, 421-449.

D. Bernache-Assolant, (1992). Biomaterials- Hard Tissue Repair and Replacement, vol. 3 (D. Muster, Editor), Elsevier, Amsterdam

Deepika Shekhawat *et al*., (2021). *IOP Conf. Ser.: Mater. Sci. Eng.* **1017** 012038**DOI** 10.1088/1757-899X/1017/1/012038.

Dowson, D., Wallbridge, N.C. (1985). Laboratory wear tests and clinical observations of the penetration of femoral heads into acetabular cups in total replacement hip joints: I: Charnley prostheses with polytetrafluoroethylene acetabular cups, Wear. 104, 203–215.

Edidin, A.A., Kurtz, S.M. (2000). Influence of Mechanical Behavior on the Wear of 4 Clinically Relevant Polymeric Biomaterials in a Hip Simulator, *Journal of Arthroplasty*, 15 321–331.

Ferry, J. D., & Morrison, P. R. (1947). Preparation and properties of serum and plasma proteins. viii. the conversion of human fibrinogen to fibrin under various conditions1, 2. *Journal of the American Chemical Society*, *69* (2), 388-400.

Ghose, D., Patra, C.N., Ravi, Kumar B.V.V., Swain, S., Jena, B.R., Choudhury, P., Shree, D. (2021). QbD-based Formulation Optimization and Characterization of Polymeric Nanoparticles of Cinacalcet Hydrochloride with Improved Biopharmaceutical Attributes. *Turkish Journal of Pharmaceutical Sciences.* 18(4), 452-464. doi:

10.4274/tjps.galenos.2020.08522. PMID: 34496552; PMCID: PMC8430414.

Ghose, D., Swain, S., Patra, C. N., Jena, B. R., & Rao, M. E. B. (2023). Advancement and Applications of Platelet-Inspired Nanoparticles: A Paradigm for Cancer Targeting. *Current Pharmaceutical Biotechnology, 24* (2), 213-237.

Giri, T.K., Thakur, D., Alexander, A., Ajazuddin, B.H., Tripathi, D.K. (2012). Alginate based hydrogel as a potential biopolymeric carrier for drug delivery and cell delivery systems: present status and applications. *Current drug-delivery,* 9, 539–5.

Goswami, C., Bhat, I.K., Patnaik, A. (2019). Fabrication of Ceramic Hip Implant Composites: Influence of Silicon Nitride on Physical, Mechanical and Wear Properties, *Silicon.*19–20. https://doi.org/10.1007/s12633-019-00222-5.

Griffith, L.G., Naughton, G. (2002). Tissue engineering– current challenges and expanding opportunities. *Science,* 295:1009–1014.

Hernigou, P., Bouthors, C. (2016). What every surgeon should know about Ceramic-on-Ceramic bearings in young patients, EFFORT. *Open Review,* 1, 107–111. https://doi.org/10.1302/2058-5241.1.000027.

Hootman, J.M., Helmick, C.G., Barbour, K.E., Theis, K.A, Boring, M.A. (2015). Updated Projected Prevalence of Self-Reported Doctor-Diagnosed Arthritis and Arthritis-Attributable Activity Limitation Among US Adults, – 2040, Arthritis Rheumatol. 68 (2016) 1582–1587. https://doi.org/10.1002/art.39692.

Jena, B.R., and Chakraborty, A. (2021). "Recent Advancement of Carbon-based Nanomaterials (CBNs)". *Acta Scientific Pharmaceutical Sciences* 5.11: 01-02.

Katari, R., Peloso, A., Zambon, J. P., Soker, S., Stratta, R. J., Atala, A., & Orlando, G. (2014). Renal bioengineering with scaffolds generated from

human kidneys. *Nephron Experimental Nephrology*, *126*(2), 119-124.

Kaushal, S., Amiel, G. E., Guleserian, K. J., Shapira, O. M., Perry, T., Sutherland, F. W., & Mayer Jr, J. E. (2001). Functional small-diameter neovessels created using endothelial progenitor cells expanded ex vivo. *Nature medicine*, *7*(9), 1035-1040.

Kim, D.K., In Kim J., Sim, B.R., Khang, G. (2017). Bioengineered porous composite curcumin/silk scaffolds for cartilage regeneration. *Materials Science and Engineering: C,* 78:571–578.

Kumar, R., Malaval, B., Antonov, M., Zhao, G. (2020). Performance of polyimide and PTFE based composites under sliding, erosive and high stress abrasive conditions. *Tribology International,* 147.106282. https://doi.org/10.1016/j.triboint.2020.106282.

Lee, C.H., Singla, A., Lee. Y. (2001). Biomedical applications of collagen. *International Journal of Pharmaceutics,* 221:1–22.

Li, Z, Ramay, HR., Hauch, K.D., Xiao, D, Zhang, M. (2005). Chitosan-alginate hybrid scaffolds for bone tissue engineering. *Biomaterials, 26*, 3919–3928.

Mckellop, H.A., Bradley, G. (1993). Evaluation of Wear in an All-Polymer Total Knee Replacement. Part 1: Laboratory Testing of Polyethylene on Polyacetal Bearing Surfaces, *Clinical Materials* 14 117–126.

Megeed, Z., Cappello, J., & Ghandehari, H. (2002). Genetically engineered silk-elastinlike protein polymers for controlled drug delivery. *Advanced drug delivery reviews*, *54*(8), 1075-1091.

Moran, E.C., Dhal, A., Vyas, D., Lanas, A., Soker, S., Baptista, P.M. (2014). Whole-organ bioengineering: current tales of modern alchemy. *Transl Res* 163:259–267.

Nanda, A., Behera, C. C., Patel, D.K., Kumar, V., Ratha, B. N., & Panda, S. (2021). Materials for Liver Regeneration, Liver-Cell Targeting, and Normal Liver Tissue Care. In *Functional Nanomaterials for Regenerative Tissue Medicines* (pp. 181-194). CRC Press.

Pchelintsev, V.V., Sokolov, A.Y. (1988). Kinetic Principles and Mechanisms of Hydrolytic Degradation of Mono- and Polyacetals-A Review, *Polymeric. Degradation, Stab.* 21 285–310.

Peng, Z., Miyanji, E. H., Zhou, Y., Pardo, J., Hettiarachchi, S. D., Li, S., ... & Leblanc, R. M. (2017). Carbon dots: promising biomaterials for bone-specific imaging and drug delivery. *Nanoscale*, *9*(44), 17533-17543.

Radulovic, L.L, Wojcinski, ZW. (2014). PTFE (Polytetrafluoroethylene; Teflon®), Third Edit, Elsevier, https://doi.org/10.1016/B978-0-12-386454-3.00970-2.

Shivani, P., Jashandeep, S., Singh, K. (2021). Ceramic biomaterials: Properties, state of the art and future prospectives. Ceramics International, Vol. 47, Issue 20, 28059-28074, ISSN 0272-8842. https://doi.org/10.1016/j.ceramint.2021.06.238.

Sofia, S., McCarthy, M.B., Gronowicz. G., Kaplan, D.L. (2001). Functionalized silk-based biomaterials for bone formation. *Journal of Biomedical Materials Research,* 54:139–148.

Vince, D. G., Hunt, J.A., & Williams, D. F. (1991). Quantitative assessment of the tissue response to implanted biomaterials. *Biomaterials*, *12*(8), 731–736. https://doi.org/10.1016/0142-9612(91)90021-2.

Wagner, D.E., Bonvillain, R.W., Jensen. T., Girard, E.D., Bunnell, B.A., Finck, C.M., Hoffman, A.M. et al. (2013). Can stem cells be used to generate new lungs? Ex vivo lung bioengineering with decellularized whole lung scaffolds. *Respirology,* 18:895–911.

Thermodynamic Parameters and Their Excess Values for Binary Mixtures of Cyclohexane and Substituted Benzenes at different frequencies

Centurion Journal of
Multidisciplinary Research
ISSN: 2395 6216 (PRINT VERSION)
ISSN: 2395 6224 (ONLINE VERSION)
Centurion University of Technology
and Management
At - Ramchandrapur
P.O. - Jatni, Bhubaneswar
Dist: Khurda – 752050
Odisha, India

Manoj Kumar Praharaj[1] and Subhraraj Panda[2]

Abstract

The ultrasonic velocity (U), density (ñ) and viscosity (ç) have been measured for the binary mixture of benzene, chlorobenzene, nitrobenzene and pyridine successively with cyclohexane at different frequencies and at temperature 318 K for different concentrations of component liquids. The experimental data of velocity, density and

[1] Department of Physics, Ajay Binay Institute of Technology, CDA-1, Cuttack, Odisha-753014, India
[2] Department of Physics, Centurion University of Technology and Management, Odisha, India
* Corresponding Author's E-mail: m_praharaj@rediffmail.com

viscosity have been used for a comparative study of the molecular interaction in the different mixtures using the calculated thermodynamic parameter and their excess values, such as excess adiabatic compressibility ($\hat{a}^E$), excess free length (L_f^E), excess free volume (V_f^E) and excess Gibb's free energy ($\ddot{A}G^E$). Variation in the above parameters for the different mixtures is indicative of the nature of the interaction between them.

KEYWORDS: Ultrasonic velocity, Gibb's free energy, free length, and free volume.

Introduction

Ultrasonic investigations of liquid mixtures, consisting of polar and non-polar components are of considerable importance in understanding the intermolecular interactions between the component molecules, which find applications in several industrial and technological processes [1-4]. In the present paper, we have studied the various thermodynamic parameters along with their excess values from the study of variation in ultrasonic velocity at different frequencies for the following binary mixtures[4-6].

Mixture - I: Cyclohexane + Benzene

Mixture - II: Cyclohexane + Chlorobenzene

Mixture - III: Cyclohexane + Nitrobenzene

Mixture - IV: Cyclohexane + Pyridine

The temperature has been maintained at a constant value (318K). Cyclohexane belongs to the group of alicyclic hydrocarbons. It is a non-polar, un-associated, inert hydrocarbon and has a globular structure. It is highly inert toward an electrophile or nucleophille at ordinary

temperature. Due to the above properties, dispersive types of interactions are possible between cyclohexane and other components. Benzene is a non-polar solvent. It is a cyclic hydrocarbon with a continuous pi bond. Chlorobenzene is a poor electron donor to the electron-seeking proton of any group[7-10]. It has a low dielectric constant and dipole moment. The chlorine atom being an electron-withdrawing atom attracts the Àelectron of benzene ring and thus a decrease of the electron density of the ring takes place. This makes the benzene ring a relatively poor electron donor to the Cyclohexane molecules. Nitrobenzene is a polar solvent with high dielectric constant and dipole moment. Hence intermolecular interaction, in this case, is large. Pyridine is a basic heterocyclic organic compound with a lower dielectric constant and dipole moment. Pyridine molecules are spherical in shape and tightly packed.

Experimental Technique

The liquid mixtures of fixed concentration (6:4) in mole fraction were prepared by taking analytical reagent grade and spectroscopic reagent grade chemicals with the minimum assay of 99.9% and obtained from E. Merck Ltd (India). The density, viscosity, and ultrasonic velocity of all liquid mixtures were measured at temperature 318K and for different frequencies 2 MHz, 4 MHz, 6 MHz, 8 MHz[11-13]. Ultrasonic velocity measurements were made using an ultrasonic interferometer (Model M-84, supplied by M/S Mittal Enterprises, New Delhi), at different temperatures and different frequencies with the accuracy of ± 0.1m s^{-1}. The measuring cell of the interferometer is a specially designed double-walled vessel with provision for temperature constancy. An electronically operated digital constant temperature bath (Model SSI-03 Spl, supplied by M/S Mittal Enterprises, New Delhi), operating in the temperature range of"10°C to 85°C with an accuracy of ±0.1°C has been used to circulate water through the outer jacket of the double-walled measuring cell containing the experimental liquid[14-16]. The densities of the

mixture were measured using a 10-ml specific gravity bottle by relative measurement method with an accuracy of ±0.01 kg·m^{-3}. The specific gravity bottle with the experimental mixture was immersed in the temperature-controlled water bath. The weight of the sample was measured using an electronic digital balance with an accuracy of ± 0.1 mg (Model: SHIMADZU AX-200, Kyoto, Japan). An Oswald viscometer (10 ml) with an accuracy of ± 0.001 Ns·m^{-2} was used for the viscosity measurement. The flow time was determined using a digital racer stopwatch with an accuracy of ± 0.1s.

Theory

Adiabatic compressibility ($\hat{a}_{ad}$)

Adiabatic compressibility the parameter which represents the ability to change the volume of a liquid sample is [17]

$$\beta_{ad} = (\rho\, U^2)^{-1} \qquad \ldots\ldots\ldots\ldots\ldots\ldots (1)$$

Intermolecular free length (L_f)

The formula for outer to outer distance between the interacting molecules

$$L_f = K\sqrt{\beta_{ad}} \qquad \ldots\ldots\ldots\ldots (2)$$

Free volume (V_f)

The free volumes of the binary mixtures have been computed using its relationship with the ultrasonic velocity and viscosity as given below

$$V_f = \left(\frac{MU}{K\eta}\right)^{\frac{3}{2}} \qquad \ldots\ldots\ldots\ldots (3)$$

Where k is a constant, which is independent of temperature and its value is 4.28 X 10^9 for all liquids.

Gibb's free energy ("5ØÜ):

The variation of „5ØIß with temperature can be expressed in the form of Eyring salt process theory [17].

$$\frac{1}{\tau} = \left(\frac{KT}{h}\right).exp\left(\frac{-\Delta G}{KT}\right)$$

The above equation can be rearranged as

$$\Delta G = 2.30KT\log\left(\frac{KT\tau}{h}\right) \quad \ldots\ldots\ldots\ldots\ldots (4)$$

Where, '5ØIß' is the viscous relaxation time, T' is the absolute temperature, K is the Boltzmann s constant and h is the Planck s constant.

Excess thermodynamic parameters

With the help of excess parameters, the extent of deviation from the ideal behaviour of binary mixture can be estimated. The difference between the thermodynamic function of mixing for a real system and the value corresponding to a perfect solution at the same temperature, pressure and composition is called the thermodynamic excess function, denoted by Y^E[18-20].

Excess value Y^E for each parameter can compute by using the general formula

$$Y^E = Y - (Y_1 X_1 + Y_2 X_2) \quad \ldots\ldots\ldots\ldots\ldots (6)$$

Where Y is the parameter under consideration, X_1 and X_2 are mole fractions of two liquids.

Excess adiabatic compressibility ($\hat{a}^E$)

The difference of the adiabatic compressibility of the mixture and the sum of the fractional contributory adiabatic compressibility of the two liquids individually is the deviation in adiabatic compressibility. At a given mole fraction it is given by

$$\text{“}\hat{a}_{ad} = \hat{a}_{ad} - (\hat{a}_{ad1} X_1 + \hat{a}_{ad2} X_2) \quad \ldots\ldots\ldots\ldots\ldots\ldots \quad (7)$$

Excess free length (L_f^E)

The excess free length can be calculated with formula

$$L_f^E = L_f - (L_{f1} X_1 + L_{f2} X_2) \quad \ldots\ldots\ldots\ldots\ldots\ldots \quad (8)$$

Result and Discussion

The experimental values of density, viscosity and velocity are presented in table-1. Calculated values of acoustic and thermodynamic parameters are presented in table-2 and 3. Excess values of the parameters are shown in table-4 and 5.

Ultrasonic velocity increases in the following order. It is maximum for mixture-I and increases from mixture-II to mixture-III and finally to mixture-IV. Since benzene and cyclohexane both are non-polar, their intermolecular interaction is weak; hence ultrasonic velocities in such mixtures are minimum. In the cyclohexane chlorobenzene mixture, the intermolecular interaction is also weak as mentioned before; hence velocity is less than that in the mixtures III and IV[21-23]. Nitrobenzene has a larger dipole moment compared to pyridine but the intermolecular interaction is weaker in mixture-III compared to mixture-IV because of steric hindrance in nitrobenzene (Nitrobenzene being a complex and big molecule). When frequency increases, velocity in each case decreases indicating weakening of intermolecular interaction.

Intermolecular free length (L_f) is maximum for mixture-I.This is obvious as the molecular interaction in this case is weakest. For the mixture-III, L_f is the next as the interaction in this case is next as expected due to steric hindrance. L_f for mixture-IV comes the next. L_f is minimum for mixture-II. Although intermolecular interaction in this case (mixture-II) is small, the molecules in the mixture fit in to each other yielding minimum intermolecular space. Excess free length (L_f^E) is positive for system-I, III and IV and decreases in the same order. Positive L_f^E indicates weak interaction. This may be due to the non-polar nature of molecules or steric hindrance or expansion in volume from additivity. However, because of comparatively stronger interaction in mixture-IV, L_f^E is positive but small. In mixture-II, L_f^E is negative[24-25]. This may be due to the fact that the molecules fit well into each other and L_f decreases in the mixture. L_f^E does not vary with frequency in all the cases.

Adiabatic compressibility (â) decreases in the following order of the mixture-I, III, IV, and II. It changes in the same way as free length changes. At low frequencies, L_f and â are small for mixture-IV compared to mixture-II but is just the opposite when frequency increases. Excess adiabatic compressibility ($â^E$) is positive for mixture-I, III and IV and decreases in the same order. $â^E$ is negative for mixture-II. $â^E$ changes in the same way as L_f^E . Free volume (V_f) at any frequency is maximum for mixture-II and decreases successively from mixture-I o III to IV. Since Lf decreases in the order mixture-I. III. IV and II, V_f should change accordingly but for system-II it is maximum. When chlorobenzene and cyclohexane are mixed, L_f is minimum. The molecules, in this case, are close to each other and the vibrations are transmitted through the molecules to a large distance increasing the apparent free volume. Free volume decreases very slowly with an increase in frequency. Excess-free volume (V_f^E) is positive for mixture-I, III and IV and decreases in that order. In case of mixture-I, positive V_f^E is due to expansion in volume because of additivity. V_f^E decreases with an increase in frequency. In

mixture-III, V_f^E is less than that in mixture-I. The interaction in system-III being stronger, the expansion is less. However, V_f^E is less in mixture-IV than system-III as the interaction in mixture-III is less compared to mixture-IV because of steric hindrance in nitrobenzene solution. In mixture-II, V_f^E is negative and becomes more and more negative as frequency increases. When molecules are subjected to larger frequencies they vibrate rapidly, increasing the interaction between the molecules, which is of dispersive type. This reduces the free volume and hence the above observation. Internal pressure is maximum for mixture-IV and then decreases in the order mixture-I, II and III at any frequency. Pyridine molecules are spherical in shape, closely packed and have a finite dipole moment. Hence the intra-molecular as well as intermolecular interaction is maximum in case of mixture-IV. In case of system-III, it is the minimum. Nitrobenzene has a high dipole moment, but the complex structure of nitrobenzene molecules leads to less intermolecular forces and for the same reason also gives a less force of cohesion[26]. Mixture-I and II show more internal pressure compared to mixture-III because of the molecular arrangement even though benzene is non-polar and dipole moment of chlorobenzene is low. Internal pressure increases very slowly with increase in frequency for mixture-I, II and III, but comparatively more in mixture-IV. This is because, when frequency increases molecular motion increases and the molecular interaction increases.

Gibb's free energy (ÄG) is maximum for mixture-III and then for mixture-IV, II & I in that order. In all the cases, ÄG increases slowly with increase in frequency. Increase in ÄG suggests shorter time for rearrangement of molecules in the mixture. This may be due to the fact that, when frequency increases, the energy imparted to the molecules expedites the rearrangement procedure. Excess Gibb's free energy ($ÄG^E$) is negative for mixture-I & II and is positive for mixture-III & IV. In mixture-I & II ÄG decreases in the mixture indicating longer time for

rearrangement of molecules[27], as the intermolecular interaction in both of them are comparatively small. In mixture-III and IV, ÄG was large and hence ÄGE is positive. In the above two mixtures, the interaction being stronger, a shorter time is required for the rearrangement of molecules in the mixture. ÄGE changes rapidly with frequency for mixture-IV.

Tabulation

TABLE – 1: Values of Density (ñ), Viscosity (ç) and velocity (U) in binary mixtures for different frequencies.

Binary mixture	Density (ρ) ($Kg.m^{-3}$)	Viscosity ηx10^{-3} ($N.s.m^{-2}$)	Velocity (U) $m.s^{-2}$			
			2 MHz	4 MHz	6 MHz	8 MHz
M-I: Ben + C.H	818.23	0.455	1168.6	1167.2	1165.1	1164.3
M-II: C. Ben + C.H	975.25	0.549	1172.1	1169.1	1166.4	1165.5
M-III: N. Ben + C.H	856.69	0.646	1170.2	1168.4	1165.1	1164.2
M-IV: Pyridine + C.H	869.56	0.571	1247.2	1238.1	1225.3	1209.4

TABLE – 2: Calculated values of â, and L_f in binary mixtures for different frequencies.

Binary mixture	Adiabatic compressibility (β x 10^{-10}) ($N^{-1}.m^2$)				Free length (L_f x 10^{-10}) (m)			
	2 MHz	4 MHz	8 MHz	8 MHz	2 MHz	4 MHz	6 MHz	8 MHz
M-I: Ben + C.H	8.949	8.971	9.003	9.014	0.608	0.608	0.609	0.610
M-II: C. Ben + C.H	7.462	7.501	7.537	7.543	0.555	0.556	0.558	0.558
M-III: N. Ben + C.H	8.524	8.549	8.584	8.608	0.593	0.594	0.595	0.596
M-IV: Pyr. + C.H	7.393	7.499	7.669	7.859	0.552	0.556	0.562	0.569

TABLE – 3: Calculated values of V_f and ÄG in binary mixtures for different frequencies.

Binary mixture	Free volume (V_f x 10^{-7}) (m^3 .mol^{-1})				Gibb's free energy (ΔG x 10^{-20} ($k.J.mol^{-1}$)			
	2 MHz	4 MHz	6 MHz	8 MHz	2 MHz	4 MHz	6 MHz	8 MHz
M-I: Ben + C.H	3.364	3.358	3.349	3.346	0.562	0.563	0.564	0.565
M-II: C. Ben + C.H	3.590	3.576	3.563	3.561	0.564	0.567	0.569	0.569
M-III: N. Ben + C.H	3.069	3.062	3.053	3.046	0.695	0.696	0.698	0.699
M-IV: Pyr. + C.H	2.663	2.635	2.591	2.544	0.578	0.584	0.594	0.605

TABLE–4: Excess values â^E and L_f^E in binary mixtures for different frequencies.

Binary mixture	Excess Adiabatic comp. (β^E x 10^{-10}) (N^{-1} .m^2)				Excess Free length (L_f^E x 10^{-10}) (m)			
	2 MHz	4 MHz	8 MHz	8 MHz	2 MHz	4 MHz	6 MHz	8 MHz
M-I: Ben + C.H	0.3138	0.3119	0.3238	0.3127	0.012	0.011	0.012	0.011
M-II: C. Ben + C.H	-0.31	-0.291	-0.274	-0.287	-0.08	-0.08	-0.07	-0.08
M-III: N. Ben + C.H	1.965	1.975	1.999	2.009	0.083	0.083	0.084	0.084
M-IV: Pyr. + C.H	0.03	0.115	0.265	0.422	0.006	0.009	0.014	0.020

TABLE – 5: Excess values V_f^E and ÄG^E in binary mixtures for different frequencies

Binary mixture	Excess Free volume (V_f^E x 10^{-7}) (m^3 .mol^{-1})				Excess Gibb's free energy (ΔG^E x 10^{-20}) ($k.J.mol^{-1}$)			
	2 MHz	4 MHz	6 MHz	8 MHz	2 MHz	4 MHz	6 MHz	8 MHz
M-I: Ben + C.H	0.944	0.943	0.938	0.94	-0.092	-0.092	-0.091	-0.092
M-II: C. Ben + C.H	0.266	0.260	0.253	0.257	-0.031	-0.031	-0.030	-0.030
M-III: N. Ben + C.H	0.391	0.388	0.382	0.379	0.072	0.073	0.074	0.074
M-IV: Pyr. + C.H	-0.451	-0.471	-0.508	-0.544	0.056	0.061	0.069	0.078

Conclusion

Variation of ultrasonic velocity with frequency in the binary mixture of cyclohexane and benzene group of liquids enabled us to study the

thermodynamic parameters and their excess values. These indicate the nature of the interaction between the components of the mixture. Although cyclohexane is nonpolar the intermolecular interaction is evident through the excess values of the thermodynamic parameters. It has been observed that, the change in velocity with change in frequency is conspicuous in mixture-IV. This leads to large variation in the parameters and their excess values with change in frequency compared to the other mixtures.

Reference

1. Manoj Kumar Praharaj and Abhiram Satapathy, (2020). *"Molecular Interaction in Binary Liquid Mixtures by Ultrasonic Technique",* Indian Journal of Natural Sciences, 10(60), 19721-19725.

2. M.K. Praharaj, A. Satapathy, P.R. Mishra and S. Mishra, (2012). *"Study of thermodynamic and transport properties of ternary liquid mixture at different frequencies"*, Journal of Chemical and Pharmaceutical Research, 4(4), 1910-1920,.

3. S Panda , (2020). *Indian J. Pharm. Educ. Res.* 54(3),630-636.

4. Manoj Kumar Praharaj and Sarmistha Mishra, (2018). *"International Journal of Interdisciplinary Research and Innovations",* 6(3), 272-278.

5. M.K. Praharaj, A. Satapathy, P.R. Mishra and S. Mishra, (2012). *"Ultrasonic studies of molecular interactions in pyridine + N-N dimethylformamide + cyclohexane ternary liquid mixtures at different temperatures",* International Journal of Chemical and Pharmaceutical Sciences, 3(3), 6-14.

6. S Panda and AP Mahapatra, (2017*). J. Pure Appl. Ultrason*. 39,83-87.

7. M.K. Praharaj, A. Satapathy, P.R. Mishra and S. Mishra, (2013). *"Ultrasonic analysis of intermolecular interaction in the mixtures of benzene*

with N.N-dimethylformamide and cyclohexane at different temperatures", Journal of Chemical and Pharmaceutical Research, 5(1), 49-56.

8. S Panda and AP Mahapatra, (2019). *Clay Res.* 38(1) 35-42

9. Subhraraj Panda and Sutapa Khuntia, (2020). *Indian Journal of Natural Sciences,* 10(60)26449-26453

10. M.K. Praharaj, A. Satapathy, P.R. Mishra and S. Mishra, (2013). *"Study of molecular interaction in mixture of n, n-dimethylformamide, cyclohexane and benzene for different frequencies of ultrasonic waves",* Golden Research Thoughts, 2(8), 1-10.

11. S Panda and AP Mahapatra., (2019). *Intern J of Innovative Tech. and Exploring Engine.* **8(11),** 742-748

12. M.K. Praharaj, A. Satapathy, P.R. Mishra and S. Mishra, (2013). *"Ultrasonic studies of ternary liquid mixtures of N-N-dimethylformamide, nitrobenzene, and cyclohexane at different frequencies at 318 K",* Journal of Theoretical and Applied Physics, 7(23).

13. S Panda and AP Mahapatra. (2018). *J. Pure Appl. Ultrason.,* **,40**,100-105

14. Subhraraj Panda and Achyuta Prasad Mahapatra, (2020). *Indian Journal of Natural Sciences,* 10(60) 26442-26448

15. Manoj Kumar Praharaj, Abhiram Satapathy, (2019). "Journal of Emerging technologies and innovative Research", 6(4),351-353.

16. D.N. Rao, A. Krishnaiah and P.R. Naidu, (1981). Acta Chim. Acad. Sci. Hung, 107(1), 49-55.

17. B. Jacobson. (1952). *J. Chem. Phys.,* 20, 927,.

18. Subhraraj Panda and Achyuta Prasad Mahapatra, (2015). Archives of Physics Research, 6 (2), 6-12

19. C.V. Suryanarayana, and J. Kuppusamy, (1976). J. Acoust. Soc. Ind., 4, 75.

20. M. K. Praharaj, (2017). International Journal of Recent Innovation in Engineering & Research, 2(5), 13-17.

21. J.d Vanderwaals, (1873). Essay on the continuity of the gaseous and liquid States London.

22. Subhraraj Panda and Shibashis Pradhan, (2020). Indian Journal of Natural Sciences, 59(10), 18340-18345

23. S. Glasstone, (1947). *Thermodynamic for chemist*, D. van Mostrand Co., Inc., Newyork, 62.

24. S Panda and AP Mahapatra. (2016). *Int. J. of Chemical and Physical Sc.*; 5(5): 15

25. S Pand ,Praharaj M. K, (2020). Indian Journal of Natural Sciences, 59(10)18552-18557

26. Subhraraj Panda, (2020). Indian Journal of Natural Sciences, 59(10), 18436-18441

S Panda, (2022). Bulgarian Journal of Physics 49(2), 136-144.

Centurion Journal of Multidisciplinary Research (India)
Volume 13 Number 1 October 2022 - March 2023